Negoro H, Shin WS, Hakamada-Taguchi R, *et al.*	Endogenous prostaglandin D_2 synthesis reduces an increase in plasminogen activator inhibitor-1 following interleukin stimulation in bovine endothelial cells.	*J.Hypertens.*	20	1347-1354	2002
Yoshida H, Takahashi M, Koshimizu M, *et al.*	Decrease in sarcoglycans and dystrophin in failing heart following acute myocardial infarction.	*Cardiovasc.Res.*	59	419-427	2003
Koizumi T, Hikiji H, Takato T, *et al.*	Cell density and growth-dependent down-regulation of both intracellular calcium responses to agonist stimuli and expression of smooth-surfaced endoplasmic reticulum in MC_3T_3-E_1 osteoblast-like cells.	*J.Biol.Chem.*	278	6433-6439	2003
Hakamada-Taguchi R, Uehara Y, Kuribayashi K, *et al.*	Inhibition of hydroxymethylglutaryl-co-enzyme a reductase reduces Th1 development and promotes Th2 development.	*Circ.Res.*	93	948-956	2003
Numabe A, Ara N, Hakamada-Taguchi R, *et al.*	Effects of the anti-platelet aggregation drug dilazep on cognitive function in Dahl salt-sensitive rats.	*Hypertens.Res.*	26	185-191	2003
Abe T, Hikiji H, Takato T, *et al.*	Targeting of iNOS with antisense DNA plasmid prevents cytokine-induced reduction of osteoblastic activity.	*Am.J.Physiol. (Endocrinol Metab).*	285	E614-E621	2003
Hori K, Shin WS, Hemmi C, *et al.*	High fidelity SNP genotyping using sequence-specific primer elongation and fluorescence correlation spectroscopy.	*Curr.Pharm. Biotechnol.*	4	477-484	2003
Kawada T, Hemmi C, Fukuda S, *et al.*	Sarcolemmal fragility secondary to the degradation of dystrophin in dilated cardiomyopathy, as estimated by electron microscopy.	*Exp.Clin.Cardiol.*	8	67-70	2003
Toyo-oka T, Kawada T, Nakata J, *et al.*	Translocation and cleavage of myocardial dystrophin as a common pathway to advanced heart failure: a scheme for the progression of cardiac dysfunction.	*Proc.Natl.Acad.Sci. USA.*	101	7381-7385	2004
Sago N, Omi K, Tamura Y, Kunugi H, *et al.*	RNAi induction and activation in mammalian muscle cells where Dicer and eIF2C translation initiation factors are barely expressed.	*Biochem.Biophys. Res.Commun.*	319	50-57	2004
Hori M, Sasayama S, Kitabatake A, *et al.*	Low-dose carvedilol improves left ventricular function and reduces cardiovascular hospitalization in Japanese patients with chronic heart failure: the Multicenter Carvedilol Heart Failure Dose Assessment (MUCHA) trial.	*Am.Heart J.*	147	324-330	2004
Ma J, Iida H, Jo T, *et al.*	Ursodeoxycholic acid inhibits endothelin-1 production in human vascular endothelial cells.	*Eur.J.Pharmacol*	505	67-74	2004
Takahashi M, Tanonaka K, Yoshida H, *et al.*	Effects of ACE inhibitor and AT1 blocker on dystrophin-related proteins and calpain in failing heart.	*Cardiovasc.Res.*	65	356-365	2005
Kawada T, Tezuka A, Ebisawa T, *et al.*	A novel scheme of dystrophin disruption for the progression of advanced heart failure.	*Biochim. Biophys. Acta*	1751	73-81	2005
Kawada T, Masui F, Kumagai H, *et al.*	A novel paradigm for the development of advanced heart failure-Assessment by gene therapy (A review).	*Pharmacol. & Therap.*	107	31-43	2005

Iida H, Jo T, Iwasawa K, *et al.*	Molecular and pharmacological characterristics of transient voltage-dependent K^+ currents in cultured human pulmonary arterial smooth muscle cells.	*Br.J.Pharmacol.*	146	49-59	2005 .
Negoro H, Shin WS, Taguchi-Hakamada R, *et al.*	Endogenous prostaglandin D_2 synthesis decreases vas cular cell adhesion molecule-1 expression in human umbilical vein endothelial cells.	*Life Sci.*			2005 (In pres s)
Takeda S, Takahashi M, Mizukami H, *et al.*	Successful gene transfer using adeno-associated virus vectors into the kidney: comparison among adeno-associated virus serotype 1-5 vectors *in vitro* and *in vivo.*	*Nephron Exp. Nephrol.*	96	e119-26	2004
Hara T, Kume A, Hanazono Y, *et al.*	Expansion of genetically corrected neutrophils in chronic granulomatous disease mice by cotransferring a therapeutic gene and a selective amplifier gene.	*Gene Ther.*	11	1370-7	2004
Matsushita T, Okada T, Inaba T, *et al.*	The adenovirus E1A and E1B19K genes provide a helper function for transfecion-based adeno-associated virus vector production.	*J Gen Virol.*	85 (Pt 8)	2209-14	2004
Uchida M, Watanabe T, Kunitama M, *et al.*	Erythropoietin overcomes imatinib-induced apoptosis and induces erythroid differentiation in TF-1/bcr-abl cells.	*Stem Cells*	22	609-16	2004
Kanazawa T, Mizukami H, Nishino H, *et al.*	Topoisomerase inhibitors enhance the cytocidal effect of AAV- HSVtk/ganciclovir on head and neck cancer cells.	*Int.J.Oncol.*	25	729-35	2004
Ueda K, Hanazono Y, Shibata H, *et al.*	High-level *in vivo* gene marking after gene-modified autologous hematopoietic stem cell progress□t- tation without marrow conditioning in non-human primates.	*Mol.Ther.*	10	469-77	2004
Takei Y, Mizukami H, Saga Y, *et al.*	Overexpression of a hybrid gene consisting of the amino-terminal fragment of urokinase and carboxyl-terminal domain of bikunin suppresses invasion and migration of human ovarian cancer cells *in vitro.*	*Int.J.Cancer.*	113	54-8	2005
Sasaki K, Inoue M, Shibata H, *et al.*	Efficient and stable Sendai virus-mediated gene trans- fer into primate embryonic stem cells with pluripoten- cy preserved.	*Gene Ther.*	12	203-10	2005
Yoshioka T, Okada T, Maeda Y, *et al.*	Adeno-associated virus vector-mediated interleukin-10 gene transfer inhibits atherosclerosis in apolipoprotein E-deficient mice.	*Gene Ther.*	11	1772-9	2004
Takatoku M, Muroi K, Kawano-YamamotoC, *et al.*	Involvement of the esophagus and stomach as a first manifestation of varicella zoster virus infection after allogeneic bone marrow transplantation.	*Intern Med.*	43	861-4	2004
Kurachi K, Kurachi S.	Molecular mechanisms of age-related regulation of genes.	*J.Thromb. Haemost.*	3	909-14	2005
Wahed MI, Watanabe K, Ma M, *et al.*	Effects of pranidipine, a novel calcium channel antagonist, on the progression of left ventricular dysfunction and remodeling in rats with heart failure.	*Pharmacology*	72	26-32	2004

Liu H, Hanawa H, Yoshida T, *et al.*	Effect of hydrodynamics-based gene delivery of plasmid DNA encoding interleukin-1 receptor antagonist-Ig for treatment of rat autoimmune myocarditis: possible mechanism for lymphocytes and noncardiac cells.	*Circulation*	111	1593-600	2005
Kanzawa N, Kondo M, Okushima T, *et al.*	Biochemical and molecu- lar biological analysis of different responses to 2, 3, 7,8-tetra-chlorodibenzo-p-dioxin in chick embryo heart and liver.	*Arch.Biochem. Biophys.*	427	58-67	2004
Hoshino D, Hayashi A, Temmei Y, *et al.*	Biochemical and immunohistochemical characterization of Mimosa annexin.	*Planta*	219	867-75	2004
Fujimi TJ, Yasuoka S, Ogura E, *et al.*	Comparative analysis of gene expression mechanisms between group IA and IB phospholipase A2 genes from sea snake Laticauda semifasciata.	*Gene*	332	179-90	2004
Kanzawa N, Yabuta H, Fujimi TJ, *et al.*	Solubility properties of a 65-kDa peptide prepared by restricted digestion of myosin with astacin-like squid metalloprotease.	*Zoolog.Sci.*	21	159-62	2004
Kanzawa N, Shintani S, Ohta K, *et al.*	Achacin induces cell death in HeLa cells through two different mechanisms.	*Arch Biochem Biophys.*	422	103-9	2004
Kanzawa N, Tatewaki S, Watanabe R, *et al.*	Expression and tissue distribution of asta-cin-like squid metalloprotease (ALSM).	*Comp.Biochem. Physiol.*	142	153-63	2005
Temmei Y, Uchida S, Hoshino D, *et al.*	Water channel activities of Mimosa pudica plasma membrane intrinsic pro-teins are regulated by direct interaction and phos- phorylation.	*FEBS Lett.*	579	4417-22	2005
Miyashita R, Tsuchiya N, Hikami K, *et al.*	Molecular genetic analyses of human NKG2C (KLRC2) gene deletion.	*Int Immunol.*	16	163-8	2004
Zheng YH, Irwin D, Kurosu T, *et al.*	Human APOBEC3F is another host factor that blocks human immunodeficiency virus type 1 replication.	*J.Virol.*	78	6073-6	2004
Doi K, Noiri E, Tokunaga K.	The association of NAD(P)H oxidase p22 phox with diabetic nephropathy is still uncertain. Millward, and Demaine.	*Diabetes Care*	27	1518-9	2004
Gu W, Ogose A, Kawashima H, *et al.*	High-level expression of the Coxsackie-virus and adenovirus receptor messenger RNA in osteosarcoma, Ewing's sarcoma, and benign neurogenic tumors among musculoskeletal tumors.	*Clin.Cancer Res.*	10	3831-8	2004
Tochigi M, Zhang X, Umekage T, *et al.*	Association of six poly-morphisms of the OTCH4 gene with schizophrenia in the Japanese population.	*Am J Med Genet B Neuropsychiat. Genet.*	128	37-40	2004
Furuya T, Hakoda M, Tsuchiya N, *et al.*	Immunogenetic features in 120 Japanese patients with idiopathic inflammatory myopathy.	*J.Rheumatol.*	31	1768-74	2004
Hitomi Y, Tsuchiya N, Kawasaki A, *et al.*	CD72 polymorphisms associated with alternative splicing modify susceptibility to human systemic lupus erythematosus through epistatic interaction with FCGR2B.	*Hum.Mol. Genet.*	13	2907-17	2004
Akesaka T, Lee SG, Ohashi J, *et al.*	Comparative study of the haplotype struc-ture and linkage disequilibrium of chro-mosome 1p36.2 region in the Korean and Japanese populations.	*J.Hum.Genet.*	49	603-9	2004

Sakurai D, Tsuchiya N, Yamaguchi A, *et al.*	Crucial role of inhibitor of DNA binding/ differentiation in the vascular endothelial growth factor- induced activation and angiogenic processes of human endothelial cells.	*J.Immunol.*	173	5801-9	2004
Ohashi J, Naka I, Patarapotikul J, *et al.*	Strong linkage disequilibrium of a HbE variant with the (AT)9(T)5 repeat in the BP1 binding site up- stream of the beta-globin gene in the Thai population.	*J.Hum.Genet.*	50	7-11	2005
Tanaka G, Matsushita I, Ohashi J, *et al.*	Evaluation of microsatel-lite markers in association studies: a search for an immune-related susceptibility gene in sarcoidosis.	*Immuno-genetics*			2005 (In press)
河田登美枝,仲澤幹雄 豊岡照彦	生体内心筋に対する遺伝子導入-拡張型心筋症の遺伝子治療-	日本薬理学雑誌	119	37-44	2002
徳永　勝士	SNP タイピング法	*Medical Science Digest*	29	172-3	2003
河田登美枝,仲澤幹雄 豊岡照彦	心不全の重症化機構 —その新しい概念—	日本薬理学雑誌	123	55-62	2004
豊岡 照彦	心不全の重症化と、その対策	日本医事新報	4171	21-32	2004

Rescue of hereditary form of dilated cardiomyopathy by rAAV-mediated somatic gene therapy: Amelioration of morphological findings, sarcolemmal permeability, cardiac performances, and the prognosis of TO-2 hamsters

Tomie Kawada*, Mikio Nakazawa†, Sakura Nakauchi‡, Ken Yamazaki‡, Ryoichi Shimamoto‡, Masashi Urabe§, Jumi Nakata‡, Chieko Hemmi‡, Fujiko Masui‡, Toshiaki Nakajima‡, Jun-Ichi Suzuki‡, John Monahan¶, Hiroshi Sato*, Tomoh Masaki‖, Keiya Ozawa§, and Teruhiko Toyo-oka‡**

‡Department of Organ Pathophysiology and Internal Medicine, Cardiovascular Medicine, University of Tokyo, Tokyo 113-0033, Japan; *Pharmacy Division, Niigata University Medical Hospital, and †Department of Medical Technology, School of Health Sciences, Niigata University, Niigata 951-8520, Japan; §Division of Genetic Therapeutics, Center for Molecular Medicine, Jichi Medical School, Tochigi 329-0498, Japan; ‖Research Institute, National Cardiovascular Institute, Suita 565-8565, Japan; and ¶Avigen, Inc., Alameda, CA 94502

Communicated by Setsuro Ebashi, National Institute for Physiological Sciences, Okazaki, Japan, December 3, 2001 (received for review October 20, 2001)

The hereditary form comprises ≈1/5 of patients with dilated cardiomyopathy (DCM) and is a major cause of advanced heart failure. Medical and socioeconomic settings require novel treatments other than cardiac transplantation. TO-2 strain hamsters with congenital DCM show similar clinical and genetic backgrounds to human cases that have defects in the δ-sarcoglycan (δ-SG) gene. To examine the long-term *in vivo* supplement of normal δ-SG gene driven by cytomegalovirus promoter, we analyzed the pathophysiologic effects of the transgene expression in TO-2 hearts by using recombinant adeno-associated virus vector. The transgene preserved sarcolemmal permeability detected *in situ* by mutual exclusivity between cardiomyocytes taking up intravenously administered *Evans blue dye and expressing the δ-SG transgene throughout life.* The persistent amelioration of sarcolemmal integrity improved wall thickness and the calcification score postmortem. Furthermore, *in vivo* myocardial contractility and hemodynamics, measured by echocardiography and cardiac catheterization, respectively, were normalized, especially in the diastolic performance. Most importantly, the survival period of the TO-2 hamsters was prolonged after the δ-SG gene transduction, and the animals remained active, exceeding the life expectancy of animals without transduction of the responsible gene. These results provide the first evidence that somatic gene therapy is promising for human DCM treatment, if the rAAV vector can be *justified for clinical use.*

In spite of a steady progress in the pharmaceutical treatment of dilated cardiomyopathy (DCM), the patient's prognosis is still poor (1). Cardiac transplantation is the most life-saving therapy of DCM at the advanced stage, although it includes a wide variety of medical and socioeconomic problems. Another potential strategy including gene therapy is urgently required (2), particularly in the infantile or juvenile cases when it is difficult to repeat cardiac transplantation along their growth. An animal model is useful for developing a new treatment. Cardiomyopathy (CM) hamster is a representative model of human hereditary CM (3) and is divided into hypertrophic CM (BIO 14.6 strain) and DCM-inbred sublines (TO-2 strain), both of which descended from the same ancestor (4). In 1997, two groups independently identified the responsible gene as δ-sarcoglycan (δ-SG) in the strain BIO 14.6 (5, 6). We also have determined the breakpoint of δ-SG gene at the intron 1 in both BIO 14.6 and TO-2 strains (6). In human cases with DCM, the similar δ-SG gene defect has been reported in four families, and one member required heart transplantation (7).

Gene therapy might be promising for the DCM treatment of hereditary origin. Both the limited area and transient duration after the *in vivo* gene transfer has disturbed a functional evaluation of the transfected hearts (8, 9). The *in vivo* transduction of normal δ-SG gene by recombinant adeno-associated virus (rAAV) has made it possible to induce both the transcript and transgene in appreciable amounts and ameliorate cardiac dysfunction up to 10 and 20 weeks (Ref. 10; Fig. 1). This vector has been proven nonpathogenic (11, 12) and has been tried for the therapy of human patients with cystic fibrosis (13) or hemophilia B (14). We hypothesized that supplementation of normal δ-SG before the onset of disease in the DCM animals by a mean of *in vivo* gene transfer may rescue the animals from the development and progression of the disease. Here, we report that an efficient rAAV-mediated δ-SG gene transfer into hearts of TO-2 hamsters resulted in a dramatic rescue of animals from developing the disease, with long-term improvements of morphological lesions, physiological indices at both the cellular and organ levels, and the prognosis.

Materials and Methods

Experimental Animals and Specific Antibodies. Normal (n = 12) and TO-2 strain hamsters (n = 50) with the early onset of DCM (4, 6, 9) were purchased from Bio Breeders (Fitchburg, MA). All of the animals were male and 5 weeks old at the gene transduction, housed under diurnal lighting, and allowed food and tap water *ad libitum*. TO-2 strain hamsters were divided into the following three subgroups: (*i*) totally untreated animals (n = 6); (*ii*) transfected by the reporter gene, Lac Z, alone (n = 24); and (*iii*) cotransfected by Lac Z and δ-SG gene with normal sequence (n = 20). Polyclonal and site-directed antibody to δ-SG was prepared in high titer with synthetic peptide (GPKAVEAYGKKFEVKT) as a specific epitope of which amino acid sequence was deduced from the cloned cDNA (6). Monoclonal antibody to β-Gal was obtained from NovoCastra, Newcastle, U.K.

Abbreviations: DCM, dilated cardiomyopathy; CM, cardiomyopathy, δ-SG, δ-sarcoglycan; rAAV, recombinant adeno-associated virus; LVDs, left ventricular systolic dimension; LVDd, left ventricular diastolic dimension; LVP, left ventricular pressure.

**To whom reprint requests should be addressed at: Second Department of Internal Medicine, Tokyo University Hospital, University of Tokyo, Hongo 7-3-1, Bunkyo-ku, Tokyo 113-0033, Japan. E-mail: toyooka-2im@h.u-tokyo.ac.jp.

The publication costs of this article were defrayed in part by page charge payment. This article must therefore be hereby marked "*advertisement*" in accordance with 18 U.S.C. §1734 solely to indicate this fact.

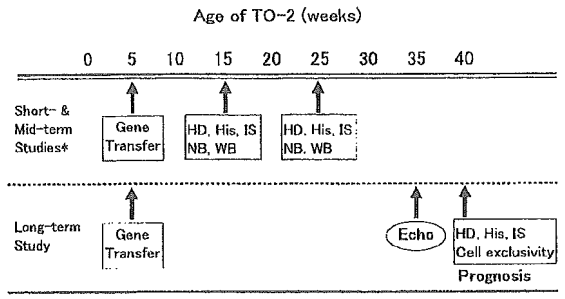

Fig. 1. Protocol for the assessment of gene therapy using rAAV vector. Unlike a previous report (10), the present study was focused mainly on the long-term efficacy and improvement of the animal's prognosis that might be the most important to verify a rationale to develop a novel therapy. HD, hemodynamics; His, histological examinations; IS, immunostaining; NB, Northern blot; and WB, Western blot.,

rAAV Vector Construction and Protocol for Gene Delivery *in Vivo*. pW1, an rAAV plasmid containing a reporter gene, Lac Z, flanked by the inverted terminal repeats of AAV genome, pHLP19, a helper plasmid with rep and cap genes, and pladeno-1, harboring adenovirus E2A, and E4 and VA genes were used for the rAAV-reporter gene production (15). pWSG harboring the δ-SG expression cassette driven by the same cytomegalovirus promoter was prepared for rAAV-δ-SG biosynthesis. These rAAVs were produced in 293 cells in culture and purified. The titer of each vector was determined, as described (10).

Under open chest surgery with constant volume ventilation (Model 683, Harvard Bioscience, South Natick, MA; ref. 10), rAAV-reporter gene (Lac Z) alone or the mixture of rAAV-Lac Z and rAAV-δ-SG gene was administered intramurally to the cardiac apex and two sites in the left ventricular free wall (10 μl each: 8.4×10^{10} and 6×10^{10} copies for Lac Z and δ-SG gene in total, respectively). Then, animals were cared for 35 weeks after the transduction in the Infection Research Laboratory under Guidance for Animal Facility: Maintenance and Housing Conditions.

The long-term protocol to follow both physiological and pathological effects *in vivo* and postmortem after the gene transfer is summarized in Fig. 1. Because the present study was addressed mainly to the examination of sarcolemmal integrity and myocardial contractility (both *in vivo*), we analyzed leaky cardiomyocytes secondary to the degradation of transmembrane dystrophin-related proteins (DRP, ref. 9) and wall motion by high-resolution echocardiography, in addition to the hemodynamic studies and prognosis analysis.

Evaluation of Pathological Alterations. The transgene expression was not restricted to the injected sites; a distant region also was transfected (10). Accordingly, wall thickness was measured at the four portions; interventricular septum, left ventricular free wall opposite to the septum, anterior and posterior free walls of the left ventricular cavity in the cross section after staining by hematoxylin and eosin and then summed. For the semiquantification of tissue calcification, we scored as follows, depending on the degree: 0 points, without calcified region; 1 point, with one calcified spot; 2 points, with two regions; and 3 points, with more than three regions and/or huge, elongated, or fused region. The score was summed in four cross sections between the apex and mitral annulus without notifying the observer as to which site and which vector was transfected.

Morphological Analyses and Evaluation of Sarcolemmal Permeability. For the immunostaining of the reporter transgene (β-Gal) and δ-SG, we used adjacent serial sections with a specific antibody to each protein because of the increased sensitivity and specificity (16). To evaluate the rAAV-δ-SG treatment, sarcolemmal integrity was analyzed by i.v. injection of 1% (vol/vol) Evans blue dye, which was kept circulating for 3 h before killing the animals at 35 weeks after the gene transduction. The dye was excluded cardiomyocytes that preserves normal sarcolemmal permeability but is taken up by the cardiomyopathic cells with leaky cell membrane (17, 18). The immunostaining of δ-SG by FITC-labeled second antibody to rabbit IgG (NovoCastra, Newcastle, U.K.) and Evans blue were visualized under double fluorescence microscopy with a Nikon F800 equipped with a green activation filter (546 nm with 12 nm band-pass) for the excitation and barrier filter (590 nm) for the emission. The site where β-Gal, a transgene of reporter, was identified by immunostaining (Fig. 2), recorded by digital camera at 200× magnification, and used for the analysis of other transgene expression or Evans blue uptake. The areas of positive cytoplasm for Evans blue or δ-SG were measured by planimetry (10) for the assay of membrane permeability and efficacy of the transduction, respectively.

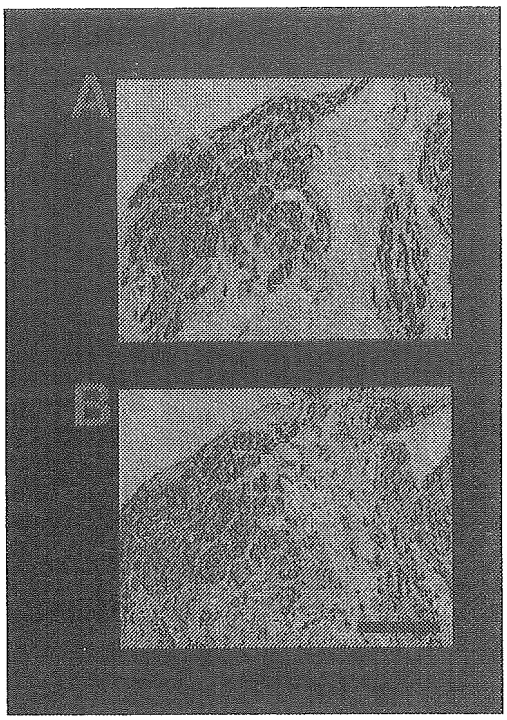

Fig. 2. Efficient expression of reporter β-Gal (*A*) or δ-SG (*B*) in serial sections after the rAAV-mediated gene transduction to the TO-2 hamster hearts that had lacked δ-SG gene (6, 9). Original magnification, ×4. (Bar = 100 μm.)

***In Vivo* Assessment of Cardiac Contractility and Hemodynamics.** Mechanical performances were determined by several observers who were not aware of the administered vectors and the injection site. Before both echocardiographic and hemodynamic measurements, the concentration of the gas anesthetic isoflurane was reduced to 1% and maintained for 20 min to stabilize the hemodynamics (19). Both the left ventricular systolic dimension (LVDs) and left ventricular diastolic dimension (LVDd) were determined by high-frequency (13 MHz) echocardiography (EUB 6000, Hitachi, Tokyo) under visualizing short axis of the left ventricle at 30 weeks after the gene transfer. Because these dimensions were still too inaccurate to determine the actual diameter of the left ventricular cavity even using the two-

dimensional view, we measured the percent fractional shortening (FS) and calculated the ejection fraction (EF) by Teicholz's formula.

Thirty-five weeks after the transduction, hamsters were anesthetized again, as described above (19). A catheter-tip transducer (SPR-671, Millar Instruments, Houston, TX) was inserted into the left ventricle through the right carotid artery to measure the left ventricular pressure (LVP), the left ventricular end-diastolic pressure (LVEDP) and the derivative of LVP (dP/dt). For the determination of the central venous pressure (CVP), a heparin-saline-filled polyethylene catheter connected to a pressure transducer was introduced into the superior vena cava through the right jugular vein. The hemodynamic parameters were recorded after A/D transduction on a Power Lab system (A. D. Instruments, Castle Hill, NSW, Australia) at a 1-kHz sampling rate (10, 19).

Evaluation of the Prognosis After Gene Therapy. The final effect of the gene therapy was evaluated on the life-saving action in the TO-2 animals ($n = 20$) with cotransduction of δ-SG plus reporter genes, comparing them with another animal group transfected by reporter gene alone ($n = 24$). All animals were operated on at age 5 weeks, randomly allocated for each treatment, and housed for 40 weeks, which exceeded the mean lifespan of TO-2 strain hamsters (4). The survival rate was evaluated by Kaplan-Meier analysis.

Statistical Analysis. Preliminary study has revealed that the morphological and physiologic effects of each gene were independent and did not show any additive or synergistic action (10). All values were expressed by the means ± SE and analyzed by paired Student's t test and ANOVA. A P value of less than 0.05 was considered significant.

Results

Wall Thickness, Calcified Lesion, and Transgene Expression. Wall thickness measured at four points of the left ventricular wall of TO-2 heart and summed revealed that the *in vivo* cotransduction of reporter and δ-SG genes ($n = 16$) increased the thickness from 4.4 ± 0.2 to 5.1 ± 0.3 mm ($P < 0.05$), compared with the heart transfected by the reporter gene alone ($n = 10$). These results confirmed previous data that cell width in the myocardium transfected by δ-SG gene was normalized, in part, by the present therapy (10).

The calcified lesion was homogeneously distributed throughout the ventricular wall at random. We semiquantitatively scored the lesion in each animal and summed. TO-2 hearts transfected by the Lac Z gene alone ($n = 10$) showed a 1.46-fold larger score than those treated by both Lac Z and δ-SG genes ($n = 16$, 9.9 ± 0.9 vs. 6.8 ± 1.0, $P < 0.05$). These results denote the physiological effect of δ-SG on the progression of calcification.

To identify the transgene of the reporter, immunostaining of β-Gal protein by specific antibody was more sensitive than the classic, histochemical reaction and did not disturb the immunodetection of SG protein secondary to blue color presentation of the reaction product after histochemistry (16). The β-Gal expression was observed at 35 weeks after the transduction (i.e., at age 40 weeks) in cardiac muscle of TO-2 hamsters. Combined with a previous report that the transgene also was documented at 10 and 20 weeks after the gene transfer (10), the present results indicate that the transgene expression with rAAV continued throughout the animal's life (4).

The transgenes of both reporter and δ-SG were clearly detected in the same part of serial sections (Fig. 2). The β-Gal was shown exclusively in the cytoplasm of cardiomyocytes (Fig. 2*A*), indicating that β-Gal did not require translocation after the biosynthesis. It should be noted that most myocardial cells presenting β-Gal matched those cells exhibiting δ-SG (Fig. 2*B*). In contrast, the expression of δ-SG was not restricted to sarcolemma, and cytoplasm in some cardiomyocytes also was stained, similar to skeletal muscle (17, 18). Furthermore, it might be quite meaningful to detect the transgene expression in ventricular working muscle cells, His-Purkinje bundle, and coronary smooth-muscle cells (Fig. 2*B*); ventricular myocytes look to be more preferentially transfected than the conduction system.

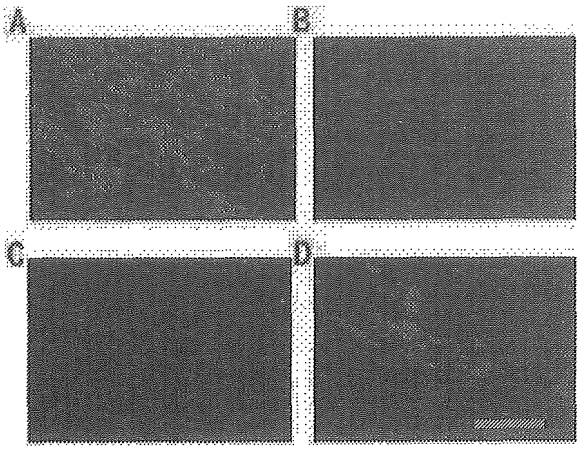

Fig. 3. Mutual cell-exclusivity of δ-SG expression and Evans blue uptake. After the cotransduction of reporter gene plus normal δ-SG gene (*A* and *B*) or transduction of the reporter gene alone (*C* and *D*) for 35 weeks to TO-2 hamster hearts, the transgene of δ-SG and the cells with leaky sarcolemma were detected by double fluorescence with FITC-labeled antibody (*A* and *C*) and Evans blue (*B* and *D*), respectively. Original magnification, ×200. (Bar = 100 μm.)

Amelioration of Sarcolemmal Permeability After the Gene Therapy. To examine the nonspecific effect of gene transfer on myocardium, the age-matched TO-2 hamsters transfected by reporter gene alone were used as controls of TO-2 hamsters cotransfected by reporter gene plus δ-SG gene. At 35 weeks after the transduction, cardiac tissue was collected and examined for δ-SG expression and Evans blue dye uptake by double fluorescence visualization. As expected, cardiac muscle from TO-2 hamsters treated by the reporter plus δ-SG genes revealed the site-specific expression of δ-SG transgene, where the reporter was detected in a serial section. The δ-SG (green fluorescence, Fig. 3*A*) was stained across cardiomyocytes that did not take up Evans blue (red fluorescence, Fig. 3*B*), distinctly showing the mutual cell-exclusivity of δ-SG expression and the dye uptake. In contrast, the TO-2 heart transfected by the reporter gene alone revealed the absence of δ-SG (Fig. 3*C*) and the extensive dye uptake (Fig. 3*D*). The control F1B heart demonstrated no uptake of Evans blue but clear immunostaining of δ-SG (data not shown).

It should be intensified that the rAAV-δ-SG treatment of TO-2 muscle achieved the protection of cardiomyocytes from sarcolemmal leakage as late as 40 weeks old, when some TO-2 hamsters died of heart failure (4). In the distant myocardium where β-Gal or δ-SG was not detected, Evans blue was strongly stained (data not shown). These results unequivocally demonstrate the physiological significance of δ-SG to protect cardiomyocytes from the sarcolemmal deterioration, similar to gene therapy for 10- and 20-week-old hamsters (10).

Quantitative assessment of the relationship between δ-SG staining and Evans blue uptake required counting every positive cell in composite photographs. These data demonstrate that Evans blue-positivity conferred a 5.88-fold protective effect of the gene therapy (20 specimens of 5 animals in each group), because the ratio decreased from 4.48 ± 0.27 to 0.83 ± 0.13 ($P < 0.01$).

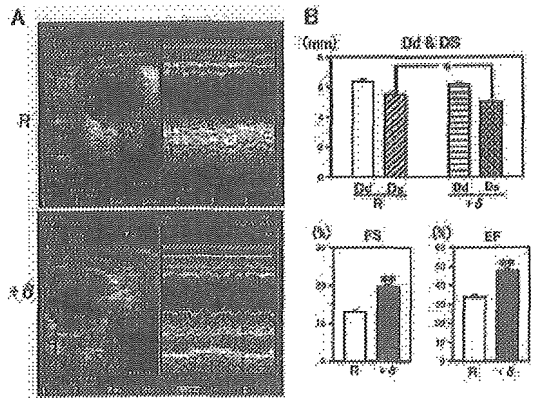

Fig. 4. (*A*) Short-axis view of the left ventricular cavity by high-frequency (13 MHz) echocardiography and M mode recording in TO-2 hamsters. The LVDs and LVDd were determined at 30 weeks after the transduction of reporter gene (R) alone or the cotransduction of R plus normal δ-SG gene (+δ) to TO-2 heart *in vivo*. (*B*) Summary of the LVDd (Dd), LVDs (Ds), fractional shortening (FS), and ejection fraction (EF) in a group transfected by the reporter gene alone (white bar, $n = 10$) or another group cotransfected by the reporter gene plus normal δ-SG genes (black bar, $n = 10$).

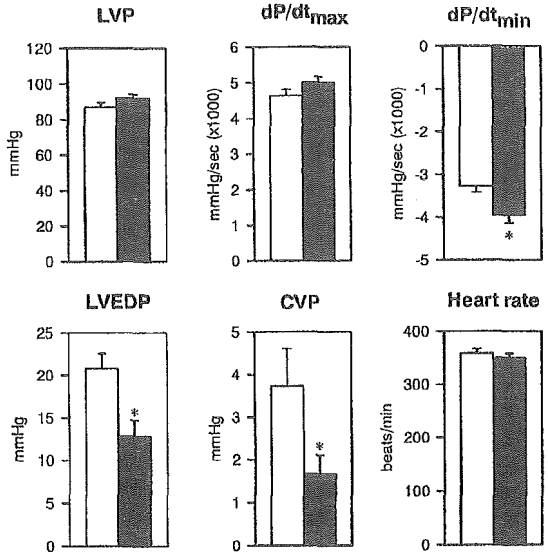

Fig. 5. Comparison of hemodynamic indices at 35 weeks after the gene transduction *in vivo*. LVP, CVP, and the heart rate were recorded under stable anesthesia (10). The LVP was digitized to calculate the maximum derivative (dP/dt_{max}) and the minimum derivative (dP/dt_{min}). White and black bars denote TO-2 hamsters transfected by the reporter gene alone (R) and cotransfected by the reporter plus δ-SG genes (+δ) for 30 weeks, respectively. *, statistical significance between the two groups ($P < 0.05$).

Improvement of Myocardial Contractility and Hemodynamic Indices. High-frequency (13 MHz) echocardiography and its digital recording have made it possible to exactly evaluate the mechanical performances *in vivo* (Fig. 4). Operation procedure at 30 weeks before (Fig. 1) did not disturb visualization of the ventricular cavity (Fig. 4*A*). The *in vivo* cotransduction of reporter gene plus δ-SG gene ($n = 10$) to the TO-2 strain reduced the enlarged LVDs from 5.52 ± 0.18 to 4.98 ± 0.09 mm ($P < 0.05$), compared with the animals ($n = 10$) transfected by the reporter gene alone (Fig. 4*B*). In contrast, the LVDd did not change even after the gene therapy in both groups (6.33 ± 0.18, vs. 6.18 ± 0.11 mm). These results were reflected in the improvement of both percent fractional shortening (FS, 12.9 ± 0.5 vs. 19.5 ± 0.7, $P < 0.01$) and the left ventricular ejection fraction after the transfer of δ-SG gene (LVEF, 33.7 ± 1.2 vs. 47.4 ± 1.3; $P < 0.01$; Fig. 4*B*).

Open chest surgery for the gene transduction did not hamper the exact measurement of the hemodynamics at 35 weeks after the gene transduction (Fig. 5). Cotransduction of both the reporter and δ-SG genes ($n = 18$) distinctly improved the dP/dt_{min} (−3,269 ± 147 vs. −3,955 ± 183 mmHg/sec, $P < 0.05$), the LVEDP (20.8 ± 1.8 vs. 12.8 ± 1.9 mmHg, $P < 0.05$) and the CVP (3.72 ± 0.88 to 1.66 ± 0.43 mmHg, $P < 0.05$), compared with transduction of the reporter gene alone ($n = 12$). Gene therapy did not modify the LVP (86.8 ± 2.6 vs. 91.7 ± 2.4 mmHg), the dP/dt_{max} (4,629 ± 186 vs. 5,000 ± 162 mmHg/sec), or the HR (358 ± 8 vs. 350 ± 8 beats per min).

Prolongation of Life Expectancy After the Gene Therapy. At 5 weeks old, one group of TO-2 hamsters ($n = 20$) was administered reporter gene alone *in vivo* and another group ($n = 24$) was cotransfected by the reporter and δ-SG genes. All animals survived the open chest surgery, indicating that the operational procedure did not cause serious effect on their mortality or morbidity.

The group treated by reporter gene alone started to die at 34 days old and the number of deceased animals gradually increased from 171 to 228 days after the gene transfer (Fig. 6). The death timing supports the previous data in the same strain without gene manipulation (4). In contrast, all animals in another group cotransfected by the reporter plus δ-SG genes survived and remained active. We conclude that the present gene therapy prolonged the survival rate ($P < 0.01$), when the gene responsible for DCM was supplemented *in vivo*.

Discussion

The present study demonstrated that, upon rAAV-mediated efficient δ-SG gene transfer into the heart, TO-2 hamsters can be rescued from developing DCM and survive for at least 40 weeks, which exceeded the lifespan of TO-2 heart without responsible gene transduction, thus drastically improving the disease prognosis.

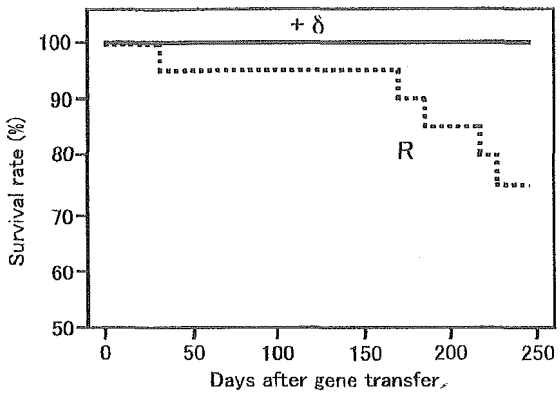

Fig. 6. Kaplan–Meier analysis of TO-2 strain hamsters' survival rate after the transduction of the reporter gene alone (R, $n = 20$) or cotransduction of the reporter plus normal δ-SG genes (+δ, $n = 24$) *in vivo*. Note that the animal group treated by R alone completely matched the prognosis of the animals without the gene manipulation (4), whereas another group treated by +δ survived the operational procedures for the *in vivo* gene transfer and remained active.

DRP links intracellular contractile machinery with extracellular matrix (20, 21). Gene defect and the corresponding protein disruption in the complex commonly induce muscle degeneration with or without cardiac symptoms. In fact, gene mutation of cardiac F-actin, dystrophin, each SG and laminin-α2 in addition to lamin A/C causes DCM in human cases as the chief symptom or a partial sign (20–23). Furthermore, acquired case in rat with myocarditis after enterovirus infection shows DCM-like symptoms secondary to the selective cleavage of dystrophin by protease 2A translated from the virus genome (24). We also have demonstrated that over-administration of isoproterenol to rats caused the selective cleavage of dystrophin, its translocation from sarcolemma to myoplasm, cardiomyocyte apoptosis, and finally acute or subacute heart failure (24). Accordingly, the interruption between intracellular F-actin and extracellular laminin-α2 would fail to preserve the integrity of sarcolemma, resulting in a DCM-like syndrome, irrespective of the hereditary or acquired origin.

Wall thickness was normalized after the gene therapy, and this fact might be a result of improved cell diameter (10) and/or the reduction of calcified lesions in the transfected site. Furthermore, the reduced calcification suggests that the pathogenesis is intrinsic to the deletion of the δ-SG gene *per se* and is not a result of additional deletions other than the δ-SG gene. Although the rAAV type 2 vector is potent for the widespread and long-lasting gene transduction *in vivo*, efficacy was still lower than the case after open chest surgery and confirms our previous results of the gene therapy for short or mid-term period (10). Other methods of gene transfer *in vivo* using intracoronary administration and/or electroporation did not exceed the present level of intramural administration (T.K., M.N., J.N., C.H., and T.T.-o., unpublished data). More efficient gene transfer through coronary circulation, as succeeded in heterotopically transplanted heart after the isolated perfusion (17), would completely restore these pathological alterations before the progression to irreversible degeneration. The apparent discrepancy between the reduced LVDs by echocardiography, and no effect on the LVP or dP/dt_{max} by hemodynamic study, might be explained by the insufficient gene delivery to cover whole heart. Escape of both atria from the gene transduction and their reduced contractility may decrease the preload of both ventricles and would not be reflected to the increment of LVP or dP/dt_{max}. We have reported that transduction of 30–40% cells and 20% protein amount were sufficient for improving hemodynamics, as was verified by immunohistology and Western blotting, respectively, for the level of δ-SG to rescue the animals (10). These results suggest the redundant expression of δ-SG in normal animals.

Based on the results of cardiomyocyte degradation in transgenic mice and their improvement by the pharmaceutical agent with coronary dilating action, K. P. Campbell and coworkers (25, 26) have presented the scheme that loss of δ- or β-SG but not α-SG would cause DCM secondary to the coronary spasm. These results are quite informative for the development of DCM, but may require further studies on the exact pathogenesis because of the following three reasons. (*i*) The same δ-SG gene deletion causes different phenotypes in hamsters; hypertrophic CM at the initial onset followed by DCM in BIO 14.6 strain (4, 6) and DCM as the first symptom in TO-2 strain (4, 6, 9, 10). It might be attractive to assume that an additional mutation in the TO-2 strain causes DCM, overcoming the compensatory hypertrophy that occurs in BIO 14.6 strain (*ii*). After the gene therapy, δ-SG was expressed in not only cardiomyocytes but also in smooth-muscle cells in the coronary artery (Fig. 2*B*). We found no significant difference in the coronary artery caliber between the δ-SG transfected and nontransfected arteries (data not shown). Measurements of local coronary flow with the vasospasm-inducing agents (e.g., acetylcholine or ergonovine) are mandatory to determine the contribution of coronary spasm (27). (*iii*) In addition, another kind of Ca^{2+} entry blocker, nifedipine, with more potent antispastic and more specific coronary dilating action (28) did not improve but rather aggravated the prognosis of this hamster (29).

Cardiac muscle is destined to repeat contraction and relaxation throughout the lifespan, and sarcolemma is supposed to be much more resistant to the expansion-shrinking cycle in the heart than in the skeletal muscle. The lack of a component in DRP is not lethal (20, 21), but its full set may be needed to keep both the membrane integrity and normal lifespan. Actually, present results demonstrate that the exogenously applied Evans blue dye permeated plasma membrane of cardiomyocytes that did not possess δ-SG (Fig. 3 *C* and *D*) when TO-2 hamsters started to die of heart failure (Fig. 6). In contrast, myocardial cells expressing δ-SG after the gene transduction did not take up the dye at the same age (Fig. 3 *A* and *B*). Continuous but gradual leakage of sarcolemma to Ca^{2+} in addition to the Ca^{2+} entry during slow inward current would elevate the intracellular Ca^{2+} level (30) because of the depletion of high-energy phosphates (31) and would activate the endogenous protease, calpain (Ca^{2+}-activated neutral protease, CANP; ref. 32). After that, α–, β– and γ-SG might be hydrolyzed at the posttranslation level (6, 9), because mRNAs for α–, β– and γ-SG were completely preserved (6), and because most of the cytoskeletal proteins, including SGs, are degraded (32) by isolated calpain (M. Koshimizu, H. Yoshida, and S. Takeo, personal communication). On the precise mechanism of DCM progression or coronary spasm, more detailed study would be required on sarcolemmal fluidity (31), humoral factors, or cytokines, including tumor necrosis factor α and/or endothelin (33, 34).

Recent data for some mice with lysosomal storage disease showed hepatocellular carcinoma or angiosarcoma were detected after intrauterine and i.v. administration of rAAV (35). In addition, we found a trace staining of β-Gal protein in liver, spleen, and kidney, suggesting extracardiac transduction of the reporter gene (S.N., T.K., and T.T.-o., unpublished data). Although species other than the transgenic animals described above did not demonstrate any tumor formation (35), and because the heart is one of the privileged organs in relation to tumorigenesis, further study is necessary to test the safety in primates. Present results distinctly indicate that somatic gene therapy with potent vector is promising for human DCM treatment, if the rAAV vector is available for clinical use.

This study was supported by grants-in-aid from the Ministry of Education, Science, Culture and Sports, the Ministry of Health, Labor and Welfare, Japan, by Uehara Memorial Foundation, and by the Motor Vehicle Foundation.

1. Packer, M., Bristow, M. R., Cohn, J. N., Colucci, W. S., Fowler, M. B., Gilbert, E. M. & Shusterman, N. H. (1996) *N. Engl. J. Med.* **334**, 1449–1355.
2. Mickels, V. V., Moll, P. P., Miller, F. A., Tajik, A. J., Chu, J. S., Driscoll, D. J., Burnett, J. C., Rodeheffer, R. J., Chesebro, J. H. & Tazelaar, H. D. (1992) *N. Engl. J. Med.* **326**, 77–82.
3. Jasmin, G., Solymoss, B. & Proschek, L. (1979) *Ann. N.Y. Acad. Sci.* **317**, 338–348.
4. Sole, M. J. (1986) *Hamster Inform. Serv.* **8**, 3–6.
5. Nigro, V., Okazaki, Y., Belsito, A., Piluso, G., Matsuda, Y., Politano, L., Nigro, G., Ventura, C., Abbondanza, C., Molinari, A. M., *et al.* (1997) *Hum. Mol. Genet.* **6**, 601–607.
6. Sakamoto, A., Ono, K., Abe, M., Jasmin, G., Eki, T., Murakami, Y., Masaki, T., Toyo-oka, T. & Hanaoka, F. (1997) *Proc. Natl. Acad. Sci. USA* **94**, 13873–13878.
7. Tsubata, S., Bowles, K. R., Vatta, M., Zintz, C., Titus, J., Muhonen, L., Bowles, N. E. & Towbin, J. A. (2000) *J. Clin. Invest.* **106**, 655–662.
8. Kawaguchi, H., Shin, W. S., Wang, Y. P., Inukai, M., Kato, M., Matsuo-Okai, Y., Sakamoto, A., Kaneda, Y. & Toyo-oka, T. (1997) *Circulation* **95**, 2441–2447.
9. Kawada, T., Nakatsuru, Y., Sakamoto, A., Koizumi, T., Shin, W. S., Okai-Matsuo, Y., Suzuki, J., Uehara, Y., Nakazawa, M., Sato, H., *et al.* (1999) *FEBS Lett.* **458**, 405–408.
10. Kawada, T., Sakamoto, A., Nakazawa, M., Urabe, M., Masui, F., Hemmi, C., Wang, Y., Shin, W. S., Nakatsuru, Y., Sato, H., *et al.* (2001) *Biochem. Biophys. Res. Commun.* **284**, 431–435.
11. Xiao, X., Li, J. & Samulski, R. J. (1996) *J. Virol.* **70**, 8098–8108.

12. Svensson, E. C., Marshall, D. J., Woodard, K., Lin, H., Jiang, F., Chu, L. & Leiden J. M. (1999) *Circulation* **99,** 201–205.
13. Wagner, J. A., Reynolds, T., Moran, M. L., Moss, R. B., Wine, J. J., Flotte, T. R. & Gardner, P. (1998) *Lancet* **351,** 1702–1703.
14. Kay, M. A., Manno, C. S., Ragni, M. V., Larson, P. J., Couto, L. B., McClelland, A., Glader, B., Chew, A. J., Tai, S. J., Herzog, R. W., *et al.* (2000) *Nat. Genet.* **24,** 257–261.
15. Fan, D. S., Ogawa, M., Fujimoto, K., Ikeguchi, K., Ogasawara, Y., Urabe, M., Nishizawa, M., Nakano, I., Yoshida, M., Nagatsu, I., *et al.* (1998) *Hum. Gene Ther.* **9,** 2527–2535.
16. Kawada, T., Shin, W. S., Nakatsuru, Y., Koizumi, T., Sakamoto, A., Nakajima, T., Okai-Matsuo, Y., Nakazawa, M., Sato, H., Ishikawa, T., *et al.* (1999) *Biochem. Biophys. Res. Commun.* **259,** 408–413.
17. Greelish, J. P., Su, L. T., Lankford, E. B., Burkman, J. M., Chien, H., Koenig, S. K., Mercier, I. M., Desjardins, P. R., Mitchell, M. A., Zheng, X. G., *et al.* (1999) *Nature Med.* **5,** 439–443.
18. Li, J., Dressman, D., Tsao, Y. P., Sakamoto, A., Hoffman, E. P. & Xiao, X. (1999) *Gene Therapy* **6,** 74–82.
19. Hirono, S., Islam, H., M. O., Nakazawa, M., Yoshida, Y., Kodama, M., Shibata, A., Izumi, T. & Imai, S. (1997) *Circ. Res.* **80,** 11–20.
20. Cox, G. F. & Kunkel, L. M. (1997) *Curr. Opin. Cardiol.* **12,** 329–343.
21. Holt, K. H., Lim, L. E., Straub, V., Venzke, D. P., Duclos, F., Anderson, R. D., Davidson, B. L. & Campbell, K. P. (1998) *Mol. Cell* **1,** 841–848.
22. Olson, T. M., Michels, V. V., Thibodeau, S. N., Tai, Y. S. & Keating, M. T. (1998) *Science* **280,** 750–752.
23. Fatkin, D., MacRae, C., Sasaki, T., Wolff, M. R., Porcu, M., Frenneaux, M., Atherton, J., Vidaillet, H. J., Jr., Spudich, S., De Girolami, U., *et al.* (1999) *N. Engl. J. Med.* **341,** 1715–1724.
24. Badorff, C., Lee, G.-H., Lamphear, B. J., Martone, M. E., Campbell, K. P., Rhoads, R. E., *et al.* (1999) *Nature Med.* **5,** 320–326.
25. Coral-Vasquez, R., Cohn, R. D., Moore, S. A., Hill, J. A., Weiss, R. M., Davison, R. L., Straub, V., Barresi, R., Bansal, D., Hrstka, R. F., *et al.* (1999) *Cell* **98,** 465–474.
26. Cohn, R. D., Durbeej, M., Moore, S. A., Coral-Vazquez, R., Prouty, S. & Campbell, K. P. (2001) *J. Clin. Invest.* **107,** R1–R7.
27. Toyosaki, N., Toyo-oka, T., Natsume, T., Katsuki, T., Tateishi, T., Yaginuma, T. & Hosoda, S. (1988) *Circulation* **77,** 1370–1375.
28. Toyo-oka, T. & Naylor, W. G. (1996) *Blood Pressure* **5,** 206–208.
29. Johnson, P. L. & Bhattacharya, S. K. (1993) *J. Neurol. Sci.* **115,** 76–90.
30. Gwathmey, J. K., Copelas, L., MacKinnon, R., Schoen, F. J., Feldman, M. D., Grossman, W. & Morgan, J. P. (1987) *Circ. Res.* **61,** 70–76.
31. Toyo-oka, T., Nagayama, K., Suzuki, J. & Sugimoto, T. (1992) *Circulation* **86,** 295–301.
32. Toyo-oka, T., Shin, W. S., Okai, Y., Dan, Y., Morita, M., Iizuka, M. & Sugimoto, T. (1989) *Circ. Res.* **64,** 407–410.
33. Torre-Amione, G. & Bozkurt, B. (1999) *Curr. Opin. Cardiol.* **14,** 206.
34. Toyo-oka, T., Aizawa, T., Suzuki, N., Hirata, Y., Miyauchi, T., Shin, W. S., Yanagisawa, M., Masaki, T. & Sugimoto, T. (1991) *Circulation* **83,** 476–483.
35. Donsante, A., Volger, C., Muzyczka, N., Crawford, J. M., Barker, J., Flotte, T., Campbell-Thompson, M., Daly, T. & Sands, M. S. (2001) *Gene Ther.* **8,** 1343–1346.

Nonselective Cation Currents Regulate Membrane Potential of Rabbit Coronary Arterial Cell

Modulation by Lysophosphatidylcholine

Kuniko Terasawa, MD; Toshiaki Nakajima, MD; Haruko Iida, MD; Kuniaki Iwasawa, MD; Hitoshi Oonuma, MD; Taisuke Jo, MD; Toshihiro Morita, MD; Fumitaka Nakamura, MD; Yoshiharu Fujimori, MD; Teruhiko Toyo-oka, MD; Ryozo Nagai, MD

Background—The effects of lysophosphatidylcholine (LPC) on electrophysiological activities and intracellular Ca^{2+} concentration ($[Ca^{2+}]_i$) were investigated in coronary arterial smooth muscle cells (CASMCs).

Methods and Results—The patch clamp techniques and Ca^{2+} measurements were applied to cultured rabbit CASMCs. The membrane potential was -46.0 ± 5.0 mV, and LPC depolarized it. Replacement of extracellular Na^+ with $NMDG^+$ hyperpolarized the membrane and antagonized the depolarizing effects of LPC. In Na^+-, K^+-, or Cs^+-containing solution, the voltage-independent background current with reversal potential (E_r) of approximately +0 mV was observed. Removal of Cl^- failed to affect it. When extracellular cations were replaced by $NMDG^+$, E_r was shifted to negative potentials. La^{3+} and Gd^{3+} abolished the background current, but nicardipine and verapamil did not inhibit it. In Na^+-containing solution, LPC induced a voltage-independent current with E_r of approximately +0 mV concentration-dependently. Similar current was recorded in K^+- and Cs^+-containing solution. La^{3+} and Gd^{3+} inhibited LPC-induced current, but nicardipine and verapamil did not inhibit it. In cell-attached configurations, single-channel activities with single-channel conductance of ≈32pS were observed when patch pipettes were filled with LPC. LPC increased $[Ca^{2+}]_i$ as the result of Ca^{2+} influx, and La^{3+} completely antagonized it.

Conclusions—These results suggest that (1) nonselective cation current (I_{NSC}) contributes to form membrane potentials of CASMCs and (2) LPC activates I_{NSC}, resulting in an increase of $[Ca^{2+}]_i$. Thus, LPC may affect CASMC tone under various pathophysiological conditions such as ischemia. ***(Circulation.* 2002;106:3111-3119.)**

Key Words: muscle, smooth ■ cells ■ ischemia ■ ion channels

Lysophosphatidylcholine (LPC), a major lysophospholipid in mammalian tissues, is formed from phosphatidylcholine by phospholipase A_2. It accumulates in myocardial tissue during ischemia[1,2] and has toxic effects on myocardium, which include electrophysiological disturbances such as a decrease in membrane potential, followed by the occurrence of arrhythmia during ischemia.[3] LPC is also known as a vasoactive phospholipid that has biological effects on arterial walls, including coronary artery.[4] The prominent mechanism for vascular effects of LPC is to impair endothelium-dependent relaxing factor–mediated vasodilation, which inhibits nitric oxide production.[5] In addition, LPC is reported to increase intracellular Ca^{2+} concentration ($[Ca^{2+}]_i$) in vascular smooth muscle cells (VSMCs) and increase vascular tone.[4,6] However, the underlying mechanisms for LPC effects on coronary arterial smooth muscle cells (CASMCs) have not been investigated.

Smooth muscle tone of arteries is an important determinant of coronary circulation and vascular resistance. Coronary arterial tone is regulated by various physiological and pathological changes such as O_2 tension and an increase of H^+, resulting in autoregulation of local blood flow. Membrane potential plays additional crucial roles in regulating arterial tone and hence arterial diameter; depolarization activates voltage-gated Ca^{2+} channels, subsequently increasing Ca^{2+} entry, which regulates muscle contractility and leads to vasoconstriction. The voltage-dependent K^+ channel (K_V) plays essential roles in forming membrane potential in VSMCs.[7] ATP-sensitive K^+ channels also regulate coronary tone under ischemia.[8] However, the membrane potential of VSMCs including CASMCs is much less than K^+ equilibrium potential,[9,10] proposing that additional membrane channels such as Cl^- may contribute to form it.[11] Alternatively, the background nonselective cation current (I_{NSC}), which forms membrane potential, is identified in cardiac myocytes[12–14] and pulmonary smooth muscle cells,[15] but it has not been reported in CASMCs.

Received June 24, 2002; revision received August 29, 2002; accepted September 2, 2002.

From the Department of Cardiovascular Medicine (K.T., T.N., H.I., K.I., H.O., T.J., T.M., F.N., T.T., R.N.), University of Tokyo, Tokyo, Japan; and the Department of Cardiology (K.T., Y.F.), Narita Red Cross Hospital, Chiba, Japan.

Correspondence to Dr T. Nakajima, Department of Cardiovascular Medicine, University of Tokyo, 7-3-1 Hongo, Bunkyo-ku, Tokyo, Japan 113-8655. E-mail masamasa@pb4.so-net.ne.jp

Circulation is available at http://www.circulationaha.org

DOI: 10.1161/01.CIR.0000039345.00481.1D

Therefore, we have investigated the effects of LPC on electrophysiological activities and $[Ca^{2+}]_i$ mobilization in rabbit CASMCs. We found that the background I_{NSC} contributes to form membrane potential of CASMCs, and LPC further induces I_{NSC}, followed by an increase in $[Ca^{2+}]_i$.

Methods

Cell Preparation

Rabbit CASMCs were grown from explants of adult male Japanese White rabbit (2.5 to 3.0 kg, n=15) coronary arteries by explants methods. They exhibited typical "hill and valley" growth patterns and exhibited positive fluorescence with antibodies against α-smooth muscle actin but no fluorescence with antibodies against factor VIII antigen. They were grown in Dulbecco's modified Eagle's medium (DMEM, Sigma) supplemented with 10% fetal bovine serum (FBS, Sigma), 100U/mL penicillin, 100 μg/mL gentamicin, and 0.25 μg/mL amphotericin B (GIBCO BRL) in a humidified atmosphere of 5% CO_2 and 95% air at 37°C. When cells became confluent, they were subcultured in the same medium with 0.5% trypsin in 0.02% EDTA. Confluent cells at passages 3 to 6 were used for the experiments.

Solutions and Drugs

The control Tyrode solution contained (in mmol/L) NaCl 136.5, KCl 5.4, $CaCl_2$ 1.8, $MgCl_2$ 0.53, glucose 5.5, and N-2-hydroxyethylpiperazine-N'-ethane sulfonic acid (HEPES)-NaOH buffer 5.5(pH 7.4). The Ca^{2+}-free Tyrode solution contained EGTA (0.5 mmol/L). The high K^+ bathing solution contained KCl 140, $CaCl_2$ 1.8, $MgCl_2$ 0.53, glucose 5.5, and HEPES-NaOH buffer 5.5 (pH 7.4). In $NMDG^+$ solutions, Na^+ was replaced with equimolar N-methyl-D-glucamine$^+$ ($NMDG^+$). In low Cl^- solutions, Cl^- was replaced with aspartate, and external concentration of Cl^-($[Cl^-]_o$) was reduced to 10 mmol/L. The K^+ internal solution in the patch pipette contained KCl 140, EGTA 5, $MgCl_2$ 2, Na_2ATP 3, GTP 0.1, and HEPES-KOH buffer 5 (pH 7.2). The Cs^+ internal solution contained CsCl 140, EGTA 5, $MgCl_2$ 2, Na_2ATP 3, GTP 0.1, and HEPES-CsOH buffer 5 (pH 7.2). The K^+, Cs^+, or Na^+ extracellular solution was as follows: KCl, CsCl, or NaCl 140, glucose 5.5, HEPES 5.5(pH 7.4). In cell-attached experiments, the Cs^+-pipette solution contained CsCl 140, $CaCl_2$ 1.8, $MgCl_2$ 0.53, HEPES 5 (pH 7.4).

Palmitoyl-L-α-lysophosphatidylcholine (LPC), lanthanum (La^{3+}), gadrinium (Gd^{3+}), verapamil, nicardipine, 4-aminopyridine (4-AP), and tetraethylammonium (TEA) were purchased from Sigma. Fura-2 acetoxymethyl ester (fura-2/AM, molecular probes) was obtained from Dojin Chemicals.

Measurements of $[Ca^{2+}]_i$

Primarily cultured CASMCs on a glass culture dish were used. At confluence, CASMCs were loaded with 4 μmol/L fura-2/AM in DMEM for 60 minutes at 37°C. After loading, cells were washed 3 times, and the medium containing fura-2/AM was removed. The glass culture dish was mounted on an inverted microscope (Diaphot TMD, Nikon). Measurement of $[Ca^{2+}]_i$ was performed with a SPEX dual-wavelength fluorolog spectrometer (SPEX Industries, Inc). Excitation wavelengths of 340 and 380 nm and an emission

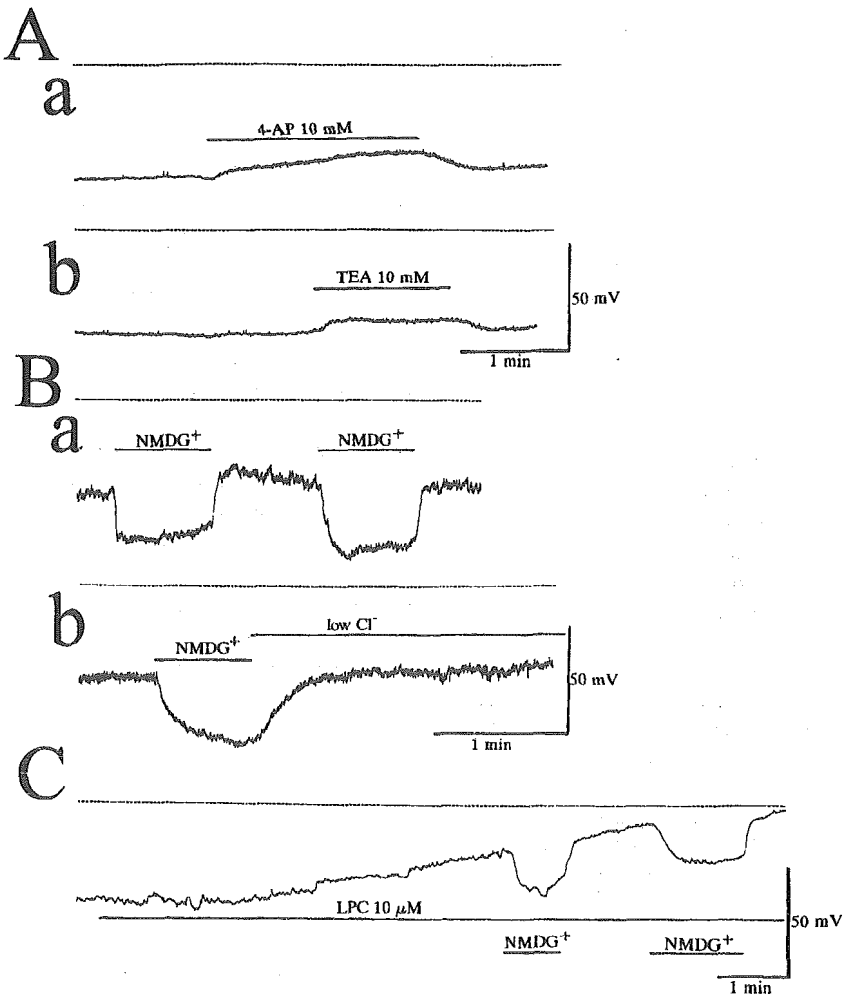

Figure 1. A, Effects of K^+ channel blockers on membrane potentials. B, Effects of replacement of Na^+ with $NMDG^+$ and reduction of Cl^-. C, Effects of LPC (10 μmol/L) on membrane potentials and replacement of Na^+ with $NMDG^+$.

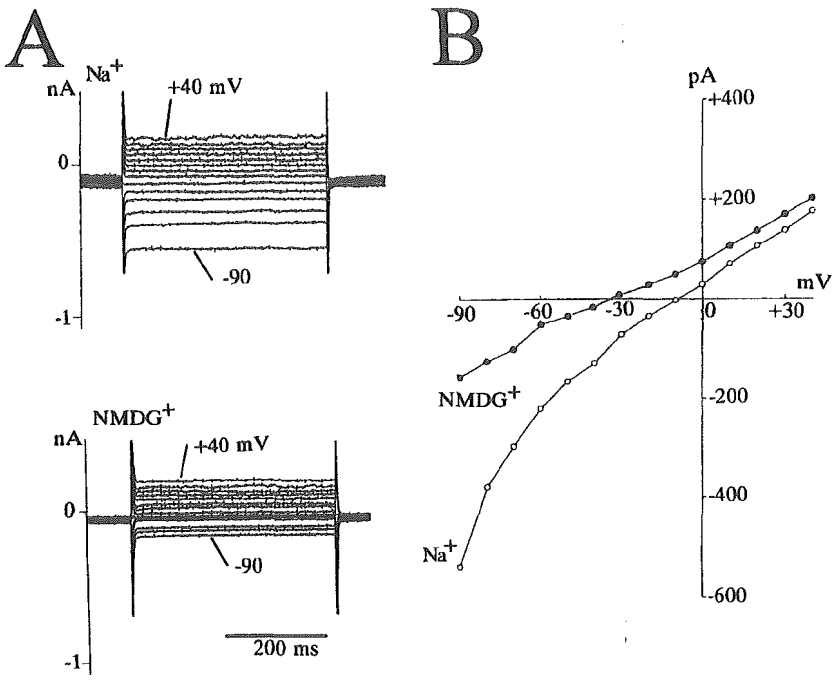

Figure 2. Effects of replacement of extracellular Na^+ by $NMDG^+$ on background current. A, Upper traces are recorded in control solution and lower traces in conditions in which Na^+ was replaced by $NMDG^+$. Results are representative of 4 similar experiments. B, Current-voltage relations measured at steady state in control and after replacement of Na^- by $NMDG^+$.

wavelength of 505 nm were used. In assessment of $[Ca^{2+}]_i$, fluorescence intensity ratio of F_{340}/F_{380} was used as an indicator of $[Ca^{2+}]_i$.[16]

Recording Technique and Data Analysis

Membrane potential and currents were recorded by using whole-cell clamp techniques.[17,18] The patch electrode had the tip resistance of 3 to 5 mol/LΩ, and series resistance was compensated. The data were reproduced, low-pass filtered at 1 kHz (−3dB) with a Bessel filter (FV-625, NF,48dB/octave slope attenuation), and sampled at 5 kHz. All data were acquired and analyzed on a Power Macintosh 7100/80 by using the PULSE+PULSEFIT software (HEKA Electronic) and Igor PRO (Wave Metrics). Single-channel currents were replayed from videotape either to a chart recorder (2400S, Gould Inc), or to the A/D broad for digitization.

Statistical data are expressed as mean±SD; n represents the number of cells tested. A Student's *t* test was used for statistical analysis, and a value of $P<0.05$ was considered significant.

Results

Membrane Potentials and Effects of LPC

With K^+ internal solution, the membrane potential was −46.0±5.0 mV (n=30). 4-AP (Figure 1Aa,10 mmol/L) depolarized the membrane potential from −51.6±4 mV to −34±6 mV (Figure 1Aa, n=4, $P<0.05$). TEA (10 mmol/L, n=4, Figure 1Ab) also depolarized it. Figure 1B illustrates the effects of replacement of extracellular Na^+ with membrane-impermeable $NMDG^+$ on membrane potentials. It hyperpolarized the membrane potential from −43±3 mV to −69±6 mV (Figure 1Ba, 1Bb, n=5, $P<0.05$) reversibly. However, the reduction of $[Cl^-]_o$ failed to hyperpolarize it (Figure 1Bb, n=4).

The effects of LPC (10 μmol/L) on membrane potential were investigated in Figure 1C. LPC gradually depolarized it from −45±4 mV to −10±6 mV (n=8, $P<0.05$). Replacement of Na^+ with $NMDG^+$ antagonized the depolarizing effects. It hyperpolarized the membrane from −8±5 mV in control to −26±6 mV in $NMDG^+$ solution (n=4, $P<0.05$). Reduction of $[Cl^-]_o$ failed to hyperpolarize it. The depolarizing effects of LPC were similarly observed at any cells of the passage numbers examined.

Background Current in Rabbit CASMCs

Figure 2 shows the effects of replacement of extracellular Na^+ by $NMDG^+$ on membrane currents. The patch pipette contained Cs^+ internal solution with 5 mmol/L EGTA and 3 mmol/L ATP to block K^+ currents and Ca^{2+}-dependent currents. The cell was held at −40 mV and the voltage pulses were applied from −90 to +40 mV. The background current without any time-dependent activation and inactivation was observed. The current-voltage relation measured at steady state is illustrated in Figure 2B. It is almost linear and crosses zero at −10 mV in Na^+-containing solution. Replacement of Na^+ by $NMDG^+$ reduced the inward current (Figure 2A) and shifted the reversal potential (E_r) toward more negative potentials. E_r was shifted from −10±5 to −38±5 mV (n=4, $P<0.05$). The amplitude of the background inward current measured at hyperpolarizing pulses of −90 mV was −120±40 pA (n=36).

Figure 3 shows the effects of La^{3+}, nicardipine, and verapamil on the background current. The cells were held at +0 mV and the command voltage pulses were applied from −90 to +60 mV. The current-voltage relations measured at steady state in the control and in the presence of La^{3+} are illustrated in Figure 3B. La^{3+} (1 mmol/L) abolished the background current reversibly. Gd^{2+} (1 mmol/L) also abolished it. However, nicardipine (10 μmol/L, Figure 3C) and verapamil (50 μmol/L, Figure 3D) reduced it at −90 mV only by −14±7% (n=4) and −6±5% (n=4), respectively.

Effects of LPC on Membrane Currents

Figure 4 illustrates the effects of LPC on membrane currents. The patch pipette contained 140 mmol/L Cs^+ internal solu-

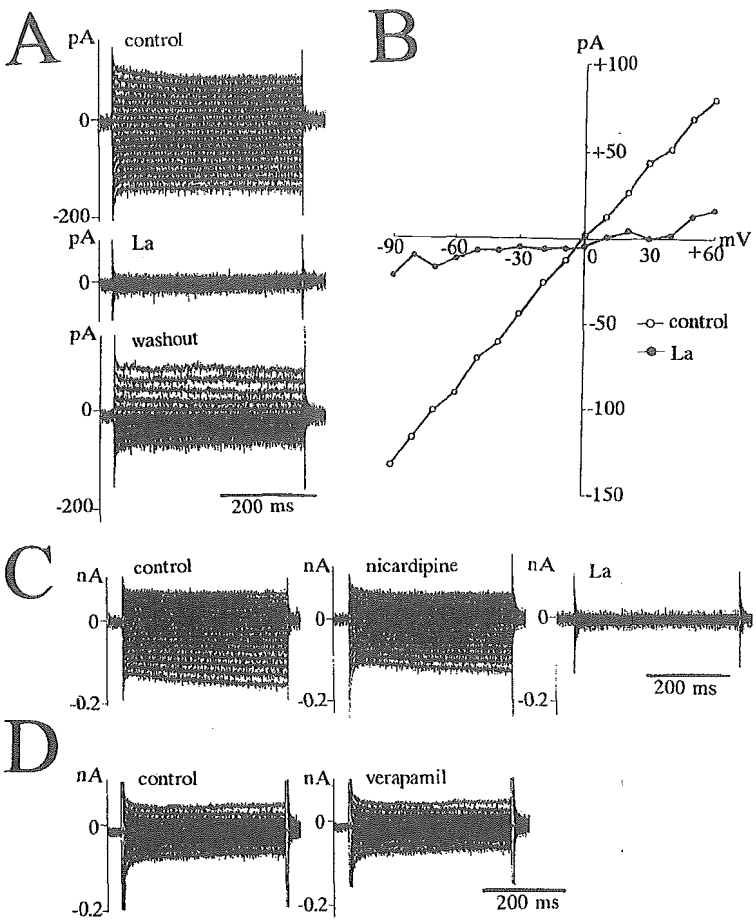

Figure 3. Background La^{3+}-sensitive currents. In A, current traces are shown in control, in the presence of La^{3+} (1 mmol/L), and after the washout. B, Current-voltage relations measured at steady state in control and in the presence of La^{3+}. C and D, Effects of Ca^{2+}-channel blockers on background current. Current traces are shown in control, in the presence of nicardipine (10 μmol/L, C), La^{3+} (1 mmol/L, C) and verapamil (50 μmol/L, D).

tion. The cell was held at −60 mV and ramp pulses from −60 to +60 mV (200 ms duration) were applied. In Figure 4A, LPC (10 μmol/L) gradually increased the inward current at a holding potential within 1 to 2 minutes and La^{3+} (1 mmol/L) completely inhibited it. Figure 4Ab illustrates the current-voltage relations in control, in the presence of LPC, and LPC plus La^{3+}. The current-voltage relation of the LPC-induced current was obtained by subtracting control current from the

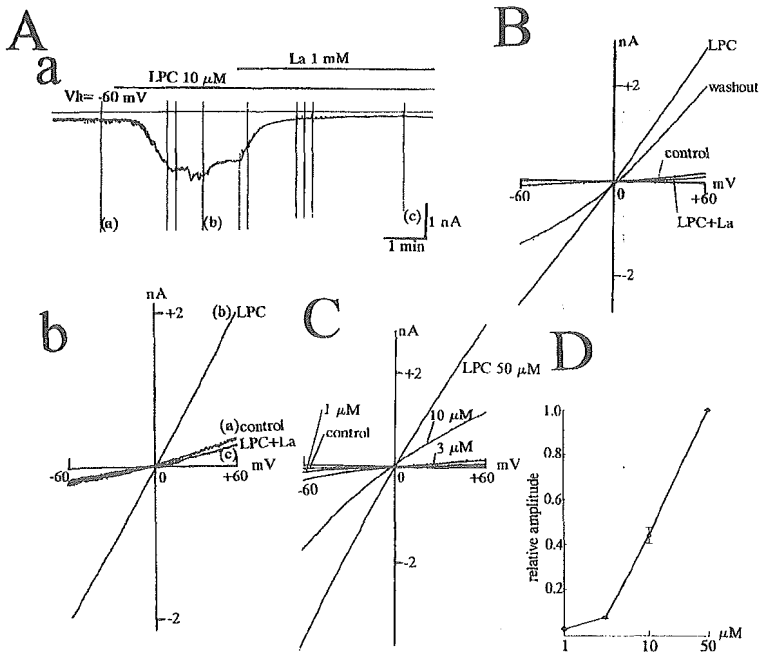

Figure 4. Effects of LPC on membrane currents. A (a, b), LPC (10 μmol/L) gradually increased the holding current into the inward direction and La^{3+} (1 mmol/L) completely inhibited it (Aa). Current-voltage relations are shown in control, in the presence of LPC, and after the addition of La^{3+} (Ab). B, Reversibility of LPC-induced current. Current-voltage relations are shown in control, in the presence of LPC, after washout, and in the presence of La^{3+}. C, Current-voltage relations in the presence of LPC (1 to 50 μmol/L). D, Current amplitude induced by 50 μmol/L LPC at −60 mV was defined as 1.0; relative current amplitude induced by LPC is plotted against each concentration. Mean±SD value obtained from 4 different cells is shown.

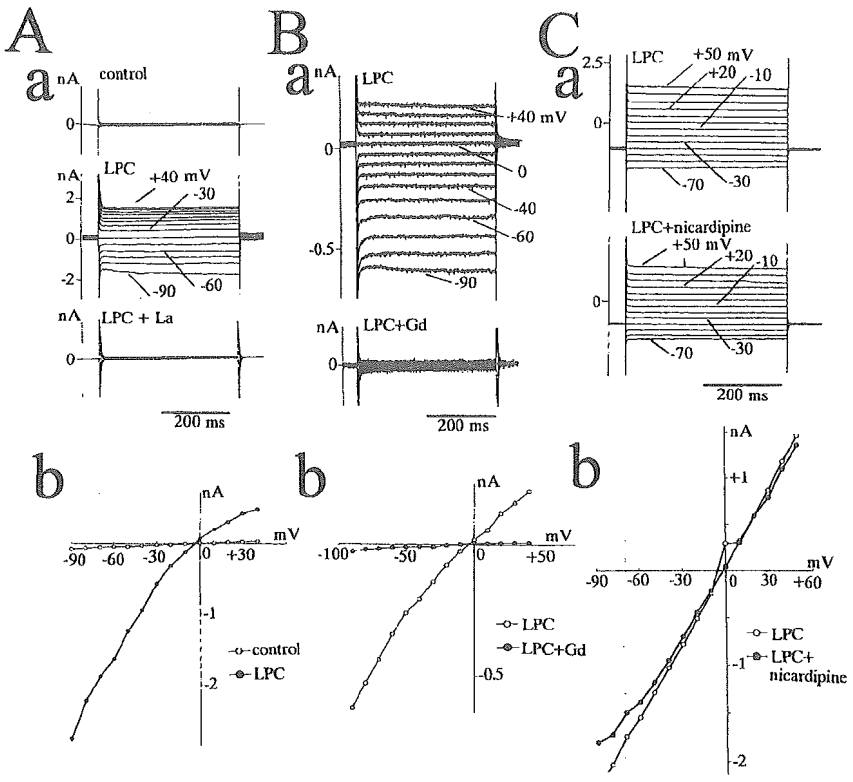

Figure 5. Effects of La^{3+} (1 mmol/L, A), Gd^{3+} (1 mmol/L, B), and nicardipine (10 μmol/L, C) on LPC-induced current. A, Current traces in control, in the presence of LPC (10 μmol/L), and LPC plus La^{3+} (a). Current-voltage relations measured at steady state in control and in the presence of LPC (b). B, Current traces in the presence of LPC and after the addition of Gd^{3+} (Ba) or nicardipine (Ca). Current-voltage relations in the presence of LPC and LPC plus Gd^{3+} (Bb) or nicardipine (Cb).

current in the presence of LPC. It was linear with E_r of approximately +0 mV. The effects of LPC (10 μmol/L) were partly reversible as shown in Figure 4B. Similar effects of LPC were observed at any cells of the passage number examined.

Figure 4, C and D show the effects of LPC (1 to 50 μmol/L) on current-voltage relations obtained by ramp pulses and dose-dependent effects of LPC. The current amplitude induced by 50 μmol/L LPC at −60 mV was defined as 1.0, and the relative current amplitude induced by LPC is plotted against each concentration. LPC concentration-dependently induced the current.

Figure 5 illustrates the effects of La^{3+}, Gd^{3+}, and nicardipine on LPC-induced current. The voltage pulses were applied from −90 to +40 mV. The cells were held at +0 mV (Figure 5, A and B) and at −40 mV(Figure 5C). The current-voltage relations measured at steady state are shown in Figure 5, Ab through Cb. La^{3+} (1 mmol/L,Figure 5A) and Gd^{3+} (1 mmol/L,Figure 5B) abolished the LPC-induced current, whereas nicardipine (10 μmol/L, Figure 5C) and verapamil (50 μmol/L) only partly inhibited it at −90 mV by −20±5% and −15±5% (n=4), respectively.

Comparative Properties of the Background and LPC-Induced Current

Figure 6 compared ionic properties of the background current with those of LPC-induced current by using ramp pulses. The background current was obtained by subtracting the current in the presence of La^{3+} from the control current. The LPC-induced current was obtained by subtracting the control current from the current in the presence of LPC (10 μmol/L). Reduction of $[Cl^-]_o$ caused no significant change of E_r on the background and LPC-induced current. E_r of background current was −6±5 and −5±5 mV (n=4, $P>0.05$) in control and low Cl^- solutions, respectively (Figure 6Aa). E_r of LPC-induced current was −2±3 and −1±3 mV (n=4, $P>0.05$) in control and low Cl^- solution, respectively (Figure 6Ab). The replacement of Na^+ by $NMDG^+$ shifted E_r of the background current from −6±5 to −31±10 mV (Figure 6Ba, n=4, $P<0.05$) and shifted E_r of the LPC-induced current from −3±3 to −16±5 mV (Figure 6Bb, n=4, $P<0.05$).

To determine cationic selectivity of the background and LPC-induced current, Na^+ was replaced by K^+ and Cs^+ (Figure 6C). The background current showed linear current-voltage relations (Figure 6Ca). E_r was +5±3 mV (n=4) in 140 mmol/L K^+ solution, +1±5 mV (n=4) in 140 mmol/L Cs^+ solution, and −8±6 mV (n=4) in 140 mmol/L Na^+ solution. The values of the slope conductance were 3.3±0.4 nS (n=4), 2.9±0.5 nS (n=4), and 2.2±0.5 nS (n=4) for K^+, Cs^+, and Na^+, respectively. The permeability ratios were calculated according to the Goldman-Hodgkin-Katz equation $E_r=RT/ZF \ln P_X[X^+]_o/P_{Cs}[Cs^+]_i$, where X^+ is Na^+, K^+, or $NMDG^+$ and F, R, T, Z have their usual meanings. $[X^+]_o$, a concentration of extracellular X^+ ion, is 140 mmol/L and $[Cs^+]_i$, a concentration of internal Cs^+ ion, is 140 mmol/L. The value of P_K/P_{Cs}, P_{Na}/P_{Cs}, and P_{NMDG}/P_{Cs}, was 1.21, 0.73, and 0.30, respectively. The LPC-induced current also showed linear current-voltage relations (Figure 6Cb). E_r was +1±4 mV (n=4), +0±3 mV (n=4), and −1±4 mV (n=4) for K^+, Cs^+, and Na^+ bathing solution, respectively. The values of the slope conductance were 40±8 nS (n=4), 35±4 nS (n=4),

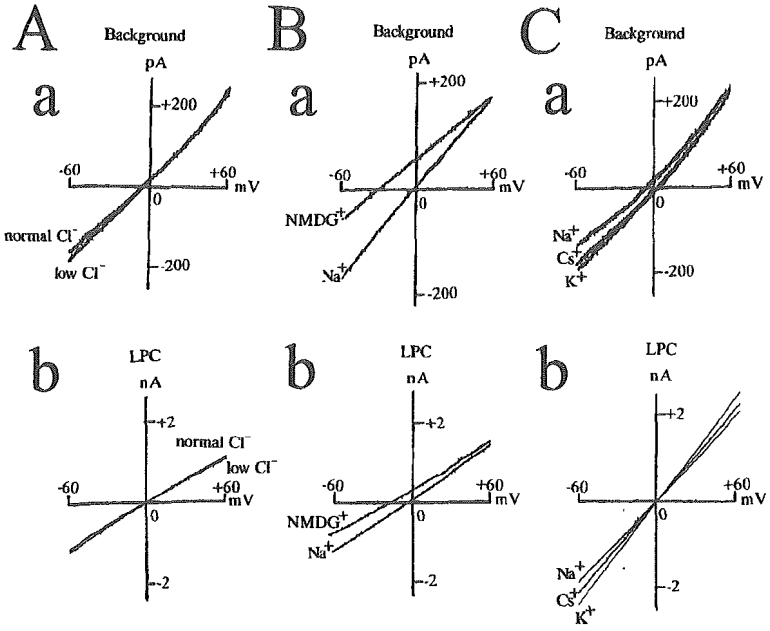

Figure 6. Effects of reduction of $[Cl^-]_o$, replacement of extracellular Na^+ by $NMDG^+$, and various monovalent cations on the reversal potential (Er) of the background and LPC-induced current. A, Effects of reduction of $[Cl^-]_o$ on Er of background (a) and LPC-induced current (b). B, Effects of replacement of Na^+ by $NMDG^+$ on Er. Na^+ was replaced by $NMDG^+$. C, Effects of various monovalent cations on Er. Current-voltage relations are indicated in various extracellular monovalent cation (Na^+, Cs^+, and K^+) solutions in the same cell.

and 33±6 nS (n=4) for K^+, Cs^+, and Na^+, respectively. The values of P_K/P_{Cs}, P_{Na}/P_{Cs}, and P_{NMDG}/P_{Cs} were 1.04, 0.96, and 0.54, respectively.

LPC-Induced Channels in Rabbit CASMCs

Figure 7 shows the results of single-channel recordings, using cell-attached methods. The patch pipette was filled with 140 mmol/L CsCl-pipette solution. The bath was perfused with high K^+ bathing solution to settle membrane potential to approximately +0 mV. Under the conditions with LPC (10 μmol/L) in the patch pipette, marked channel activities were observed at a holding potential of −100 mV (lower trace), as compared with the control (upper trace). Figure 7B shows the amplitude histogram of LPC-induced channel, which was fitted by a sum of gaussian distribution using the least-squares method. The single channel amplitude measured at −100 mV was −3.4 pA. The current-voltage relations of LPC-induced channel are illustrated in Figure 7, C and D. The relations show linearity and slope conductance of 34 pS in this cell, and E_r was approximately +0 mV. The mean slope conductance was 32±5 pS (n=4).

Effects of LPC on $[Ca^{2+}]_i$

Figure 8 shows the effects of LPC on $[Ca^{2+}]_i$. In Ca^{2+}-free solution, LPC (50 μmol/L) did not affect $[Ca^{2+}]_i$ significantly (Figure 8A). The addition of Ca^{2+} induced a sustained rise of $[Ca^{2+}]_i$, which was abolished by the removal of Ca^{2+} from the extracellular solution. The effects of LPC on $[Ca^{2+}]_i$ were

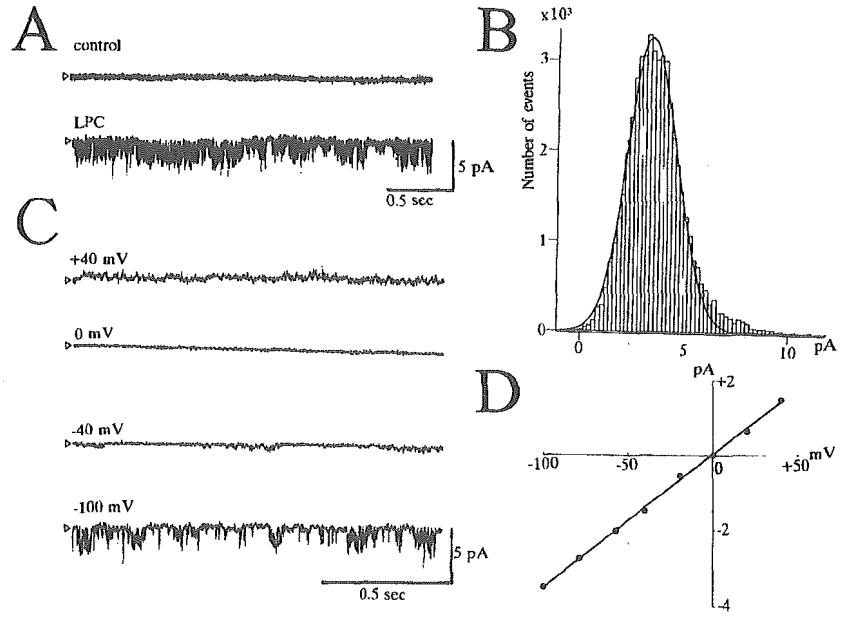

Figure 7. Activation of a specific type of channel by LPC under cell-attached modes. A, Patch pipette contained 140 mmol/L CsCl pipette solution without (control) and with LPC (10 μmol/L). Membrane potential was held at −100 mV. B, Amplitude histograms. C and D, Current-voltage relations of single LPC-activated channel.

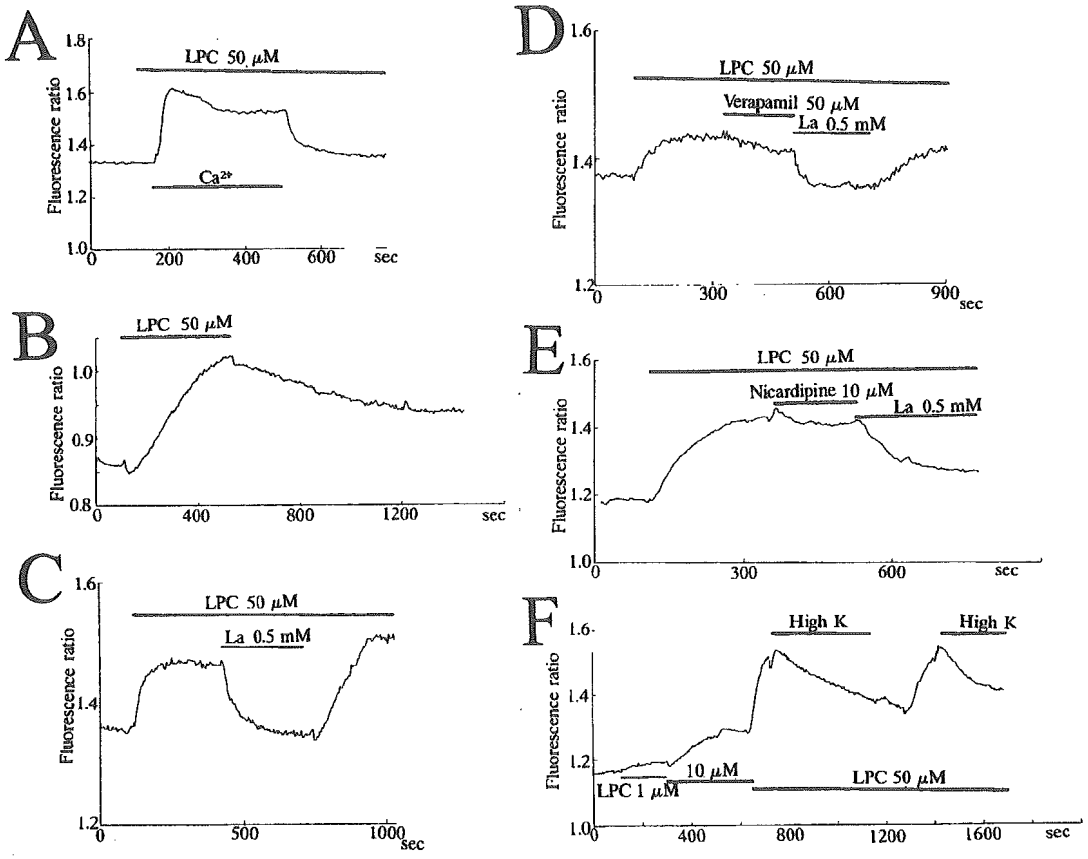

Figure 8. Effects of LPC on $[Ca^{2+}]_i$. A, Effects of LPC (50 μmol/L) on Ca^{2+} mobilization. B, Reversibility of LPC (50 μmol/L) effects. C, Effect of La^{3+} (0.5 mmol/L) on LPC-induced $[Ca^{2+}]$ rise. D and E, Effects of verapamil (50 μmol/L), nicardipine(10 μmol/L), and La^{3+} (0.5 mmol/L) on LPC-induced $[Ca^{2-}]_i$ rise. F, Concentration-dependent effects of LPC on $[Ca^{2+}]_i$ and effects of high K^+ on LPC-induced $[Ca^{2+}]_i$ rise.

partly reversible (Figure 8B). La^{3+} (0.5 mmol/L, Figure 8C) blocked LPC-induced, sustained $[Ca^{2+}]_i$ rise. However, verapamil (50 μmol/L, Figure 8D) and nicardipine (10 μmol/L, Figure 8E) partly inhibited it by −30±6% (n=3) and −19±7% (n=3), respectively. LPC (1 to 50 μmol/L) concentration-dependently increased $[Ca^{2+}]_i$ (Figure 8F). Similar results were obtained from 4 different cells. To investigate whether LPC-induced $[Ca^{2+}]_i$ rise is related to membrane potential, the bathing solution was changed from 5.4 to 140 mmol/L K^+ solution to settle membrane potential to approximately +0 mV. LPC-induced $[Ca^{2+}]_i$ rise was decreased (Figure 8F).

Discussion

Voltage-dependent K^+ current (K_V) regulates vascular tone and forms membrane potential in VSMCs, including CASMCs.[19] In our experimental conditions, 4-AP and TEA, K^+ channel blockers that produce coronary spasm,[20] inhibited K_V and resulted in depolarizing the membrane. The membrane potential has been reported to be −56±2 mV and to 40.4±4.9 mV in canine and porcine CASMCs.[9,10] It was −46.0±5.0 mV in cultured CASMCs. These values were less than K^+ equilibrium potential of approximately −80 mV, suggesting that additional membrane channels contribute to form membrane potential. The contribution of Cl^- currents has been reported in VSMCs.[11] In our study, however, reduction of $[Cl^-]_o$ failed to affect the membrane potential, whereas replacement of Na^+ by $NMDG^+$ markedly hyperpolarized it. These results suggest that the contribution of Cl^- current is minimal, and the background I_{NSC} contributes to form membrane potential in rabbit CASMCs.

The role of I_{NSC} has been investigated in pacemaking cells of hearts[12,13] and cardiac myocytes,[14] where the background Na^+ current is important to generate action potentials by raising resting membrane potential to the threshold for activation of Ca^{2+} current. The background I_{NSC} of rabbit CASMCs had the same tendencies of linear current-voltage relations and permeability sequences ($K^+ > Cs^+ > Na^+$) as the properties of the background I_{NSC} described previously[12–15] and may play important roles in forming membrane potentials as reported in pulmonary VSMCs.[15] Depolarization through I_{NSC} may open voltage-operated Ca^{2+} channels and subsequently increase $[Ca^{2+}]_i$, which regulates muscle contractility and leads to vasoconstriction.

The activation of the background I_{NSC} was not mediated by $[Ca^{2+}]_i$ rise because it was still observed under the conditions with high EGTA in the patch pipette. Similar Ca^{2+}-independent properties were observed in the background I_{NSC} of cardiac myocytes and pulmonary VSMCs,[12–15] though they were different from that reported in other cells.[21]

I_{NSC} has been reported to be activated by membrane stretch.[22] Here, we provided evidence that LPC was a potent activator of I_{NSC} in rabbit CASMCs, which was consistent with previous studies of whole-cell clamp conditions showing that LPC induced I_{NSC} in guinea pig ventricular myocytes and dog renal VSMCs.[23,24] The effects of LPC on I_{NSC} were not dependent on the passage number, and similar effects were observed in cultured cells of any passage number and freshly isolated CASMCs (data not shown). In our study, the ionic permeability ratio of K^+, Cs^+, Na^+, and $NMDG^+$ of the LPC-induced current was 1.04, 1.00, 0.96, and 0.54, which showed the same tendencies as the previous study using renal VSMCs.[24] However, it does not seem to be the same I_{NSC} reported in cardiac myocytes by Magishi et al,[23] because $NMDG^+$ passed the channel similarly as Na^+ and K^+, and Gd^{3+} did not inhibit it. Thus, it is likely that there are several types of LPC-induced I_{NSC}, depending on cell types investigated. Actually, the present study provided direct evidence showing that LPC activated a specific type of channels. However, further studies with single-channel analysis are needed to clarify the characteristic and molecular mechanisms underlying the activation of I_{NSC} by LPC.

Corr et al[3] reported that LPC was increased during ischemia, and the concentration of LPC corresponded to 990 μmol/L. In addition, atherosclerotic arteries have been reported to be chronically exposed to high concentrations of LPC as compared with normal arteries.[25,26] Thus, LPC may accumulate under pathophysiological conditions such as ischemia and atherosclerosis. Our results indicate that LPC at concentrations of 1 to 50 μmol/L induced I_{NSC}, depolarized the membrane, and resulted in $[Ca^{2+}]_i$ rise. Thus, the effects of LPC observed in this study may play significant roles in pathophysiological conditions such as ischemia.

LPC increased $[Ca^{2+}]_i$ in rabbit CASMCs, which was consistent with the previous studies in ASMCs or cardiac myocytes.[27,28] LPC may increase $[Ca^{2+}]_i$ through an increase of Ca^{2+} entry or release from Ca^{2+} storage sites. In the absence of extracellular Ca^{2+}, it failed to increase $[Ca^{2+}]_i$, suggesting that LPC increased Ca^{2+} influx as reported in rat ASMCs.[28,29] Several mechanisms by which LPC might influence $[Ca^{2+}]_i$ have been proposed. The $[Ca^{2+}]_i$ increase induced by LPC may relate to detergent or toxic effects of this amphiphile.[29] However, we used low concentrations of LPC (<50 μmol/L), and cell viability measured by trypan blue exclusion was not changed in between control and LPC-treated cells. Moreover, La^{3+} and Gd^{3+} completely abolished it, suggesting that detergent action of LPC is not likely. LPC depolarized the membrane, proposing that LPC increased $[Ca^{2+}]_i$ indirectly through voltage-dependent L-type Ca^{2+} channels. Actually, nicardipine and verapamil partly inhibited LPC-induced $[Ca^{2+}]_i$ rise. However, La^{3+} and Gd^{3+} abolished it, suggesting that LPC increased $[Ca^{2+}]_i$ mainly by activating Ca^{2+} entry pathways other than L-type Ca^{2+} channels. In our study, including single-channel analysis, LPC activated I_{NSC} with a large amplitude of approximately −1 nA at around -50 mV near resting membrane potential. La^{3+} and Gd^{3+} inhibited both the activation of I_{NSC} by LPC and LPC-induced $[Ca^{2+}]_i$ rise. In addition, when cells were bathed with high K^+ solution to settle the membrane potential to approximately +0 mV, LPC-induced $[Ca^{2+}]_i$ rise was decreased. These observations also support that LPC increased $[Ca^{2+}]_i$ through activation of I_{NSC}.

LPC has been reported to increase cGMP-dependent verapamil-sensitive $[Ca^{2+}]_i$ in ASMCs.[28] However, verapamil (50 μmol/L) and nicardipine (10 μmol/L) only partly inhibited LPC-induced $[Ca^{2+}]_i$ rise, proposing that verapamil-sensitive Ca^{2+} influx pathways do not largely contribute to $[Ca^{2+}]_i$ rise induced by LPC. The discrepancy among these results may depend on different concentrations of LPC or different cell types. LPC enhances cell proliferation and migration of CASMCs.[29,30] Since $[Ca^{2+}]_i$ is known to be related to cell proliferation and migration, activation of I_{NSC} by LPC may play essential roles in these events as well as CASMC tone.

In conclusion, I_{NSC} plays important roles in forming membrane potentials of CASMCs and LPC induces I_{NSC} and then depolarizes the membrane, resulting in an increase of $[Ca^{2+}]_i$. Thus, LPC may affect CASMCs tone under various pathophysiological conditions such as ischemia.

References

1. Sobel BE, Corr PB, Robinson AK, et al. Accumulation of lysophosphoglycerides with arrhythmogenic properties in ischemic myocardium. *J Clin Invest.* 1978;62:546–553.
2. Das DK, Engelman RM, Rousou JA, et al. Role of membrane phospholipids in myocardial injury induced by ischemia and reperfusion. *Am J Physiol.* 1986;251:H71–H79.
3. Corr PB, Snyder DW, Lee BI, et al. Pathophysiological concentrations of lysophosphatides and the slow response. *Am J Physiol.* 1982;243:H187–H195.
4. Bergmann SR, Ferguson TB Jr, Sobel BE. Effects of amphiphiles on erythrocytes, coronary arteries, and perfused hearts. *Am J Physiol.* 1981;240:H229–H237.
5. Flavahan NA. Atherosclerosis or lipoprotein-induced endothelial dysfunction: potential mechanisms underlying reduction in EDRF/nitric oxide activity. *Circulation.* 1992;85:1927–1938.
6. Suenaga H, Kamata K. Marked dissociation between intracellular Ca^{2+} level and contraction on exposure of rat aorta to lysophosphatidylcholine. *Eur J Pharmacol.* 1999;378:177–186.
7. Jackson WF. Potassium channels and regulation of the microcirculation. *Microcirculation.* 1998;5:85–90.
8. Xu X, Lee KS. Characterization of the ATP-inhibited K^+ current in canine coronary smooth muscle cells. *Pflugers Arch.* 1994;427:110–120.
9. Harder DR, Belardinelli L, Sperelakis N, et al. Differential effects of adenosine and nitroglycerin on the action potentials of large and small coronary arteries. *Circ Res.* 1979;44:176–182.
10. Sumimoto K, Hirata M, Kuriyama H. Characterization of [^{3}H]nifedipine binding to intact vascular smooth muscle cells. *Am J Physiol.* 1988;254:C45–C52.
11. Nelson MT, Conway MA, Knot HJ, et al. Chloride channel blockers inhibit myogenic tone in rat cerebral arteries. *J Physiol.* 1997;502:259–264.
12. Hume JR, Giles W. Ionic currents in single isolated bullfrog atrial cells. *J Gen Physiol.* 1983;81:153–194.
13. Hagiwara N, Irisawa H, Kasanuki H, et al. Background current in sino-atrial node cells of the rabbit heart. *J Physiol.* 1992;448:53–72.
14. Mubagwa K, Stengl M, Flameng W. Extracellular divalent cations block a cation non-selective conductance unrelated to calcium channels in rat cardiac muscle. *J Physiol.* 1997;502:235–247.
15. Bae YM, Park MK, Lee SH, et al. Contribution of Ca^{2+}-activated K^+ channels and non-selective cation channels to membrane potential of pulmonary arterial smooth muscle cells of the rabbit. *J Physiol.* 1999;514:747–758.
16. Grynkiewicz G, Poenie M, Tsien RY. A new generation of Ca^{2+} indicators with greatly improved fluorescence properties. *J Biol Chem.* 1985;260:3440–3450.

17. Hamill OP, Marty A, Neher E, et al. Improved patch-clamp techniques for high-resolution current recording from cells and cell-free membrane patches. *Pflugers Arch.* 1981;391:85–100.
18. Nakajima T, Iwasawa K, Oonuma H, et al. Troglitazone inhibits voltage-dependent calcium currents in guinea pig cardiac myocytes. *Circulation.* 1999;99:2942–2950.
19. Volk KA, Matsuda JJ, Shibata EF. A voltage-dependent potassium current in rabbit coronary artery smooth muscle cells. *J Physiol.* 1991; 439:751–768.
20. Iwaki M, Mizobuchi S, Nakaya Y, et al. Tetraethylammonium induced coronary spasm in isolated perfused rabbit heart: a hypothesis for the mechanism of coronary spasm. *Cardiovasc Res.* 1987;21:130–139.
21. Ehara T, Noma A, Ono K. Calcium-activated non-selective cation channel in ventricular cells isolated from adult guinea-pig hearts. *J Physiol.* 1988;403:117–133.
22. Zhang YH, Youm JB, Sung HK, et al. Stretch-activated and background non-selective cation channels in rat atrial myocytes. *J Physiol.* 2000;523: 607–619.
23. Magishi K, Kimura J, Kudo Y, et al. Exogenous lysophosphatidylcholine increases non-selective cation current in guinea-pig ventricular myocytes. *Pflugers Arch.* 1996;432:345–350.
24. Jabr RI, Yamazaki J, Hume JR. Lysophosphatidylcholine triggers intracellular calcium release and activation of non-selective cation channels in renal arterial smooth muscle cells. *Pflugers Arch.* 2000;439:495–500.
25. Portman OW, Soltys P, Alexander M, et al. Metabolism of lysolecithin in vivo: effects of hyperlipemia and atherosclerosis in squirrel monkeys. *J Lipid Res.* 1970;11:596–604.
26. Vidaver GA, Ting A, Lee JW. Evidence that lysolecithin is an important causal agent of atherosclerosis. *J Theor Biol.* 1985;115:27–41.
27. Woodley SL, Ikenouchi H, Barry WH. Lysophosphatidylcholine increases cytosolic calcium in ventricular myocytes by direct action on the sarcolemma. *J Mol Cell Cardiol.* 1991;23:671–680.
28. Stoll LL, Spector AA. Lysophosphatidylcholine causes cGMP-dependent verapamil sensitive Ca^{2+} influx in vascular smooth muscle cells. *Am J Physiol.* 1993;264:C885–C893.
29. Chen Y, Morimoto S, Kitano S, et al. Lysophosphatidylcholine causes Ca^{2+} influx, enhanced DNA synthesis and cytotoxicity in cultured vascular smooth muscle cells. *Atherosclerosis.* 1995;112:69–76.
30. Kohno M, Yokokawa K, Yasunari K, et al. Induction by lysophosphatidylcholine, a major phospholipid component of atherogenic lipoproteins, of human coronary artery smooth muscle cell migration. *Circulation.* 1998;98:353–359.

Original Article

The Relationship between Changes in Normal-Range Systolic Blood Pressure and Cognitive Function in Middle-Aged Healthy Women

Rie HAKAMADA-TAGUCHI*, Yoshio UEHARA*,**, Tomokazu HAEBARA***, Hideyuki NEGORO**, and Teruhiko TOYO-OKA*,**

Little is known about the effect of normal-range blood pressure (BP) on cognitive function. In previous studies investigating the relationship between BP and cognitive function in elderly subjects, underlying cerebrovascular damage has complicated the interpretation of results. To reveal the relationship between BP levels that were within an absolutely normal range and cognitive function, we examined cognitive function in normotensive, healthy middle-aged women. BP levels were measured on three separate occasions at 1-month intervals, and the subjects exhibiting normotension (<140/90 mmHg) throughout the evaluation period were recruited as normotensive subjects. Cognitive function was assessed using subtests of the Wechsler Adult Intelligence Scale—Revised. The study demonstrated that, among the subtests examined, the scores on the Digit Symbol Test, an index of psychomotor performance, had a significant correlation with normotensive-range systolic blood pressure (SBP) ($r=-0.51$, $p<0.05$); this relation was negative—that is, higher but still normal-range SBP levels were associated with impaired Digit Symbol Test scores. In addition, the relationship adjusted by age and educational level was also significant (partial correlation$=-0.56$, $p<0.05$). In contrast, diastolic BP was not related to the Digit Symbol Test ($r=-0.33$, $p=0.13$). Furthermore, the Digit Symbol Test was not influenced by blood glucose or serum cholesterol levels. These findings suggested that, even within the normotensive range, lower levels of SBP might be protective against impairment of psychomotor speed in middle-aged women. (*Hypertens Res* 2002; 25: 565–569)

***Key Words*: systolic blood pressure, cognitive function, Digit Symbol Test, psychomotor speed**

Introduction

Impairment of cognitive function in the elderly is an area of great concern across the world. Cognitive dysfunction impairs the abilities of daily life and reduces participation in social activities through deterioration in memory, attention, perception, mental flexibility, and psychomotor performance. More seriously, cognitive impairment can progress to dementia (*1*). In addition, for all of the above reasons, subjects with cognitive dysfunction require substantial assistance from their families and societies in order to support their daily lives.

Hypertension is well related to cognitive deterioration. In addition, a recent large clinical trial, the Syst-Eur trial, has demonstrated that blood pressure (BP) reduction in systolic hypertension is associated with an approximately 50% decrease in dementia (*2*). Unfortunately, however, how far BP should be lowered to achieve the greatest benefits in terms of protection of cognition remains to be answered.

From the *Health Service Center, **Department of Medicine, and ***Department of Educational Psychology, the University of Tokyo, Tokyo, Japan.
This study was partly supported by a Grant-in-Aid for Scientific Research from the Ministry of Education, Science, Sports, and Culture, Japan, and by a grant from the Japan Osteoporosis Foundation.
Address for Reprints: Rie Hakamada-Taguchi, Ph.D., Health Service Center, the University of Tokyo, 7-3-1 Hongo, Bunkyo-ku, Tokyo 113-0033, Japan. E-mail: taguchi-hec@h.u-tokyo.ac.jp
Received March 6, 2002; Accepted in revised form April 15, 2002.